CHALMERS
UNIVERSITY OF TECHNOLOGY

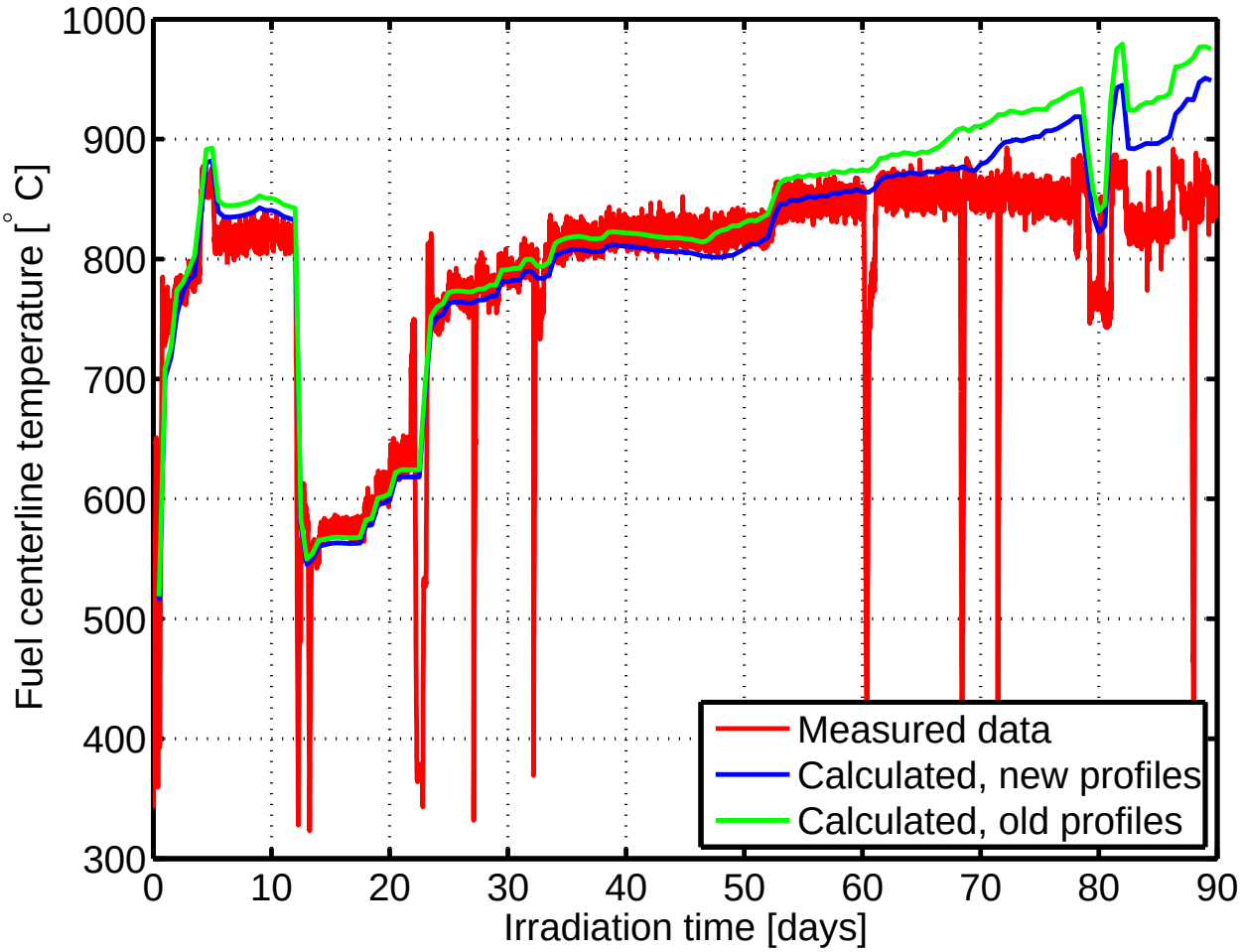

Determination of Radial Power Profiles in Thorium-Plutonium Mixed Oxide Fuel Pellets

Master's thesis in Nuclear engineering

Patrik Fredriksson

Department of Applied Physics
CHALMERS UNIVERSITY OF TECHNOLOGY
Gothenburg, Sweden 2014
CTH-NC-298
ISSN 1653-4662

MASTER'S THESIS

Determination of Radial Power Profiles in Thorium-Plutonium Mixed Oxide Fuel Pellets

Patrik Fredriksson

©Patrik Fredriksson, 2014

Supervisor: Klara Insulander Björk, Chalmers, Thor Energy AS

Examiner: Christophe Demazière, Chalmers

Department of Applied Physics
Division of Nuclear Engineering
Chalmers University of Technology
SE-412 96 Gothenburg
Sweden
Telephone: +46 (0)31-772 1000

The image on the front page illustrates the by FRAPCON calculated centre line temperature in a fuel pin along with measurement from the Halden research reactor.

Gothenburg, Sweden 2014
CTH-NT-298
ISSN 1653-4662

Abstract

To be able to license fuel for use in commercial nuclear reactors its thermomechanical behavior needs to be well known. For this, fuel performance codes need to be developed. The work described in this thesis was performed for the Norwegian company Thor Energy, and focuses on rewriting a subroutine calculating the radial power profile in the well-established fuel performance code FRAPCON so that it applies to thorium-plutonium mixed oxide fuel.

This was done by extending the previous model, by introducing some nuclides important to the thorium fuel cycle, and remaking the calculation procedure of the neutron flux. The introduction of new nuclides imposed a need for adding new effective cross sections and for updating the existing ones in the code. Due to the large amount of cross sections and other parameters a genetic algorithm was used. Data for the genetic algorithm were gathered using a Monte Carlo-based reactor physics simulation code called Serpent. Several pin configurations were simulated with different radii, plutonium content and plutonium vector.

The genetic algorithm found a set of cross sections which described the radial power profile very well for light water reactor conditions. A mean relative error of 0.57 % was observed. For halden boiling water reactor conditions the result was not equally good, with a mean relative error of 1.58 %, but was considered adequate for the present purpose. Implementing the new subroutine in FRAPCON improved the code's predictive capacity for fuel pellet centerline temperatures, as indicated by benchmarking against an experimental data set.

Keywords: Thorium, MOX, Fuel pin, Power profile, Burnup

Sammanfattning

För att licensiera ett bränsle för användning i en kommersiell reaktor så behöver dess termokemiska uppförande vara välkänt. För detta behöver bränsleprestandakoder skrivas. Arbetet beskrivet i denna tesen utfördes för det norska företaget Thor Energy, och fokuserar på att skriva om en subrutin som beräknar den radiella effektprofilen i det väletablerade bränsleprestandakoden FRAPCON så att den kan hantera toriumplutonium-oxid-bränsle.

Detta utfördes genom att utöka den tidigare modellen genom att introducera några nuklider viktiga för toriumbränslecykeln och göra om beräkningsproceduren av neutronfluxet. Introduktionen av nya nuklider påtvingade behovet att lägga till nya effektiva tvärsnitt och uppdatera de redan existerande i koden. På grund av den stora mänden tvärsnitt och andra parametrar så användes en genetisk algoritm. Data för den genetiska algoritmen samlades in med en Monte Carlo-baserad reaktorfysiksimuleringskod vid namn Serpent. Flera stavkonfigurationer simulerades med olika radie, plutoniummängd och plutoniumvektor.

Den genetiska algoritmen hittade en uppsättning tvärsnitt som beskriver den radiella effektprofilen mycket väl för LWR. Ett medelvärde på det relativa felet på 0.57 % observerades. För HBWR var resultatet inte lika bra, med ett relativt fel på 1.58 %, men detta ansågs tillräckligt bra för sitt syfte. Implementationen av den nya subrutinen i FRAPCON förbättrade kodens förutsägelse för centrumtemperaturen, som visades genom ett benchmarktest mot en experimentell datamängd.

Nyckelord: Torium, MOX, Bränslestav, Effektprofil, Utbränning

Acknowledgements

I would like to thank the people at the division of nuclear engineering where I did my work. Especially Klas Jareteg for helping me with Serpent and much of the Monte Carlo principles, Lennart Norberg for the help with all my computer and server problems. I would like to direct particular thanks to Klara Insulander Björk, my supervisor, for helping me with FRAPCON, the report and many other problems and Christophe Demazière, my examiner, for help with neutron calculations.

Göteborg, May, 2014
Patrik Fredriksson

NOTATION

Abbreviations

Reactors

BWR	boiling water reactor
PWR	pressurised water reactor
LWR	light water reactor (includes BWRs and PWRs)
HWR	heavy water reactor
HBWR	halden boiling water reactor

Materials

Th	thorium
Pu	plutonium
UOX	uranium oxide (fuel)
MOX	mixed oxide (fuel)
Th-MOX	thorium mixed oxide (fuel)

Quantities

bu	burnup [GWd/tHM]
R_O	outer radius of fuel pin [cm]
R_I	inner radius of fuel pin [cm]
σ_c	microscopic capture cross section [barn]
σ_f	microscopic fission cross section [barn]
ϕ	neutron flux [n$\cdot$ cm$^{-2}\cdot$ s^{-1}]

Contents

1 INTRODUCTION **1**
- 1.1 Context . . . 1
- 1.2 Background . . . 1
- 1.3 Purpose . . . 1
- 1.4 Scope . . . 2
- 1.5 Research questions . . . 2

2 THEORY **3**
- 2.1 Computer codes . . . 3
  - 2.1.1 FRAPCON . . . 3
  - 2.1.2 Serpent . . . 3
- 2.2 Some fissile and fertile elements . . . 4
  - 2.2.1 Plutonium . . . 4
  - 2.2.2 Thorium . . . 5
  - 2.2.3 Uranium . . . 8
- 2.3 Self-shielding . . . 8
- 2.4 FRAPCON's procedure . . . 9
  - 2.4.1 Calculation of local atomic densities . . . 10
  - 2.4.2 Approximation of neutron flux . . . 13
  - 2.4.3 Calculation of power profile . . . 16
- 2.5 Genetic Algorithm . . . 16
  - 2.5.1 Initialization . . . 17
  - 2.5.2 Evaluation . . . 17
  - 2.5.3 Selection . . . 17
  - 2.5.4 Crossover . . . 17
  - 2.5.5 Mutation . . . 18
  - 2.5.6 Replacement and Elitism . . . 18
  - 2.5.7 Application of a GA . . . 18
  - 2.5.8 Experiment design . . . 19
- 2.6 Monte Carlo simulation . . . 20

2.6.1 Statistical properties . . . 20
2.6.2 Particle simulation . . . 21
2.6.3 Model . . . 21
2.6.4 Approach by Serpent . . . 21
2.6.5 Advantages and disadvantages . . . 22

3 METHODS **23**
3.1 Working procedure . . . 23
3.2 Sensitivity analysis . . . 23
3.2.1 Results of sensitivity analysis . . . 24
3.2.2 Discussion of the sensitivity analysis . . . 25
3.3 Reference data generation . . . 26
3.3.1 Pin model . . . 26
3.3.2 Reference cases . . . 28
3.4 Parameter determination . . . 29

4 RESULTS **31**
4.1 Serpent simulation . . . 31
4.2 Parameter values . . . 34
4.3 The new model . . . 37
4.3.1 Statistics . . . 40
4.3.2 Comparison with experimental data . . . 43

5 DISCUSSION **45**
5.1 Serpent simulation . . . 45
5.2 Parameter values (GA) . . . 47
5.3 The TTPBRN model . . . 49
5.4 Comparison with experimental data . . . 50
5.5 Further work . . . 50

6 CONCLUSIONS **51**

Bibliography **53**

Appendix **54**
A Reference cases . . . 54
B Sensitivity analysis cases . . . 60
C Initial guesses . . . 63

1

INTRODUCTION

1.1 Context

In order for a fuel to be licensed its properties must be fully known. Furthermore, it must be possible to predict them during normal operation and possible transients of the reactor. There exist fuel performance codes for this, but codes for thorium fuels are very limited since they have never been used for commercial power production. Thor Energy is a Norwegian company with head office in Oslo. Their main field is to develop thorium fuel for light water reactor (LWR) conditions and software to predict the behaviour for this new fuel. One part of the work done by Thor Energy is to establish a code, an altered version of FRAPCON, as a part of the licensing process for thorium fuel and this thesis is a part of that work.

1.2 Background

Today all commercial nuclear reactors use uranium as fuel, sometimes mixed with plutonium to create mixed oxide (MOX) fuel as in many reactors in Europe and especially in France [1]. There are however ideas of using thorium instead of uranium in the MOX fuel, creating Th-MOX fuel, as this mixture has some better properties. These properties include higher net consumption of plutonium as it is not produced by the thorium itself as the case with uranium by the (n,γ) reaction. Thorium waste has good properties as it is highly insoluble, non-oxidizable and good at retaining the fission products and higher actinides inside the fuel lattice [2].

1.3 Purpose

The purpose of the work done by Thor Energy is to enable the licensing of thorium fuel for use in commercial operating power plants. This master thesis focuses at a specific

part of this project, namely the prediction of the radial power profile of the fuel rods. A subroutine predicting this profile is developed/rewritten, taking into consideration several aspects of the fuel, including but not limited to, the dimensions of the fuel pin, the power history and the composition of the fuel. The power profile is important due to its strong coupling to the temperature and to the fission gas release and thus the safety. Due to the difference in both absorption and fission cross sections for the fertile and fissile isotopes in the Th-MOX fuel compared to the uranium fuel, the radial power profile is expected to behave differently, and some extra consideration is needed.

1.4 Scope

The scope of the project includes rewriting a subroutine in FRAPCON called TUBRNP (TransUranus BuRNuP model), and the two functions TURBIN and TURBO strongly coupled to it. These will incorporate thorium as the main fuel instead of uranium. To do this some other codes need to be used, and this is described more in detail in Section 2.1.

1.5 Research questions

This thesis investigates the following research questions:

- How do the radial power profiles in thorium-plutonium mixed oxide fuel differ from those in uranium oxide fuel?
- How can they be determined using a simple and rapid algorithm?

2

THEORY

2.1 Computer codes

Several computer codes were used during the project for various purposes. FRAPCON is the main code of the project, and the goal is to implement new subroutines into it. Serpent is used to create reference data for the purpose of determining the unknown parameters introduced by the new subroutines.

2.1.1 FRAPCON

FRAPCON is a computer code written in Fortran-90, developed by the Pacific Northwest National Laboratory for the U.S Nuclear Regulatory Commision. It calculates the steady-state behaviour of oxide fuel rods for high burnup, up to 62 GWd/tHM. It calculates the thermal-mechanical behaviour, including the temperature, pressure and fuel rod deformation [3]. One specific model is the TUBRNP model, which uses the burnup and atomic densities to calculate the radial power profile. This subroutine is called repeatedly during the execution of FRAPCON and thus can not be computationally heavy.

FRAPCON has been validated for boiling and pressurized water reactors with both heavy and light water moderator. Both Uranium OXide (UOX) and uranium-plutonium Mixed Oxide (MOX) fuel, with and without gadolinium, can be simulated with the code.

2.1.2 Serpent

Serpent is a three-dimensional continuous-energy Monte Carlo reactor physics burnup calculation code [4], developed at VTT Technical Research Centre of Finland. It uses a universe-based combinatorial solid geometry model (CSG) for the description of the geometry of the system. The geometry is built up of volumes constrained by surfaces and bodies, such as spheres and cuboids. Each volume is assigned a material, described

in material cards. The material cards define the composition of the material, the temperature and some other physical properties. More advanced geometries, such as fuel pins and spherical fuel pellets and also lattices for several different reactor geometries are available.

For nuclear interactions, such as (n,γ) or (n,f) reactions, Serpent uses Ace format data libraries with continuous-energy cross sections. Interactions are based on ENDF reaction files, which describes for example distribution of emitted particles and charged-particle production [5], classical collision kinematics and probability table sampling. Cross section data is available for 6 temperatures, equally distributed between 300 and 1800 K and methods for treating the Doppler-broadening between these temperatures exist. Particular thermal scattering data are also available for heavy water, light water and graphite.

Burnup calculation in Serpent is based on built-in routines and does not depend on any external coupling. To determine changes in isotopic composition due to irradiation (burnup), Serpent solves the standard Bateman depletion equations. This is done with the Chebyshev Rational Approximation Method (CRAM), which is an advanced matrix exponential method.

2.2 Some fissile and fertile elements

In most commercial reactors today uranium is used as fuel. Usually less than 5 % of the uranium is the fissile isotope ^{235}U and the rest ^{238}U, which is a fertile isotope. Thorium mixed oxide fuel (Th-MOX) fuel uses thorium and plutonium instead of uranium and these elements have some different properties than uranium, affecting the properties of the fuel pins they are a constituent of. Thermal cross sections in the following sections refer to the cross sections at 0.0253 eV.

2.2.1 Plutonium

Plutonium is a transuranic element and has atomic number 94 in the periodic table between neptunium and americium. It does not exist naturally, but is present in the biosphere because of the atmospheric nuclear weapon tests in the 50s and 60s [6]. Plutonium is produced by neutron capture in ^{238}U in nuclear reactors, followed by two consecutive β decays. There are 5 major isotopes of plutonium to be considered in reactor applications, $^{238-242}$Pu. All of these are alpha emitters except ^{241}Pu, which is a beta emitter. Isotopes 239 and 241 are fissile and 238 and 240 are fertile.

Plutonium is divided into two groups, characterized by the composition of plutonium isotopes. A composition with less than 8 % ^{240}Pu is considered weapon grade plutonium and a composition with more than 19 % ^{240}Pu is considered reactor grade plutonium [6]. All isotopes of plutonium are created and burned continuously in thermal reactors. If the reactor operates to a burnup of only 100 MWd/tHM, in contrast to 45 000 MWd/tHM [6] for normal LWR fuel, weapon grade plutonium can be extracted. As the burnup increases there is a build up of higher plutonium isotopes, making it unreliable and

hazardous for use as bomb material. It can still be utilized for power production, hence the name reactor grade plutonium.

Plutonium is sometimes added to fresh fuel to create MOX fuel. This is done for two reasons, partly to use the plutonium produced during operation as a by-product, which can not be utilized during normal operation. There are also plans in the USA to use weapon grade plutonium for MOX fuel for the purpose of destroying the nuclear warheads produced during the cold war. Russia also has a program for burning weapon grade plutonium is some of their reactors [7].

The thermal fission and capture cross sections of the plutonium isotopes are shown in Table 2.1. ^{239}Pu and ^{241}Pu both have a larger fission cross section than ^{235}U and all isotopes have a quite high capture cross section.

Table 2.1: The thermal absorption and fission cross sections of the important plutonium isotopes [8].

Isotope	Fission cross section [barn]	Capture cross section [barn]
^{238}Pu	17	510
^{239}Pu	752	270
^{240}Pu	~ 0.059	290
^{241}Pu	1010	370
^{242}Pu	< 0.2	19

2.2.2 Thorium

Thorium is an actinide with the atomic number 90, next to actinium and protactinium. There exists only one isotope in nature, ^{232}Th, which is fertile. It can be transmuted into ^{233}U by neutron capture and two subsequent β-decays. Thorium is about three times more abundant than uranium in the earth's crust [9], making it a resource worth being considered.

Compared to ^{238}U, ^{232}Th has a larger thermal capture cross section, 7.37 barn compared to 2.7 barn [8]. Another difference is the resonance absorption by epithermal neutrons. For thorium, this resonance range is narrower and the intensity weaker, see Figure 2.1. These two things result in an overall higher capture rate, but less concentrated to the rim in a fuel pin environment. The higher capture rate will generate a lower power output in the centre of the pin at the beginning of the irradiation, leading to a lower centerline temperature, which is desirable. There will also be less high burnup structure on the fuel pin rim due to lower breeding of fissile material at the rim for high burnup, which might increase the discharge burnup of the fuel. Since thorium does not have any fissile isotope by its own, a fissile driver needs to be added before it can be used as a fuel. This can be either ^{235}U, ^{233}U or as in the case of Th-MOX fuel, reactor or weapon grade plutonium.

As plutonium is not produced by thorium during irradiation, the addition of pluto-

nium as a fissile driver can be a method to destroy unwanted stockpiles of plutonium, both from old fuel and weapon grade plutonium.

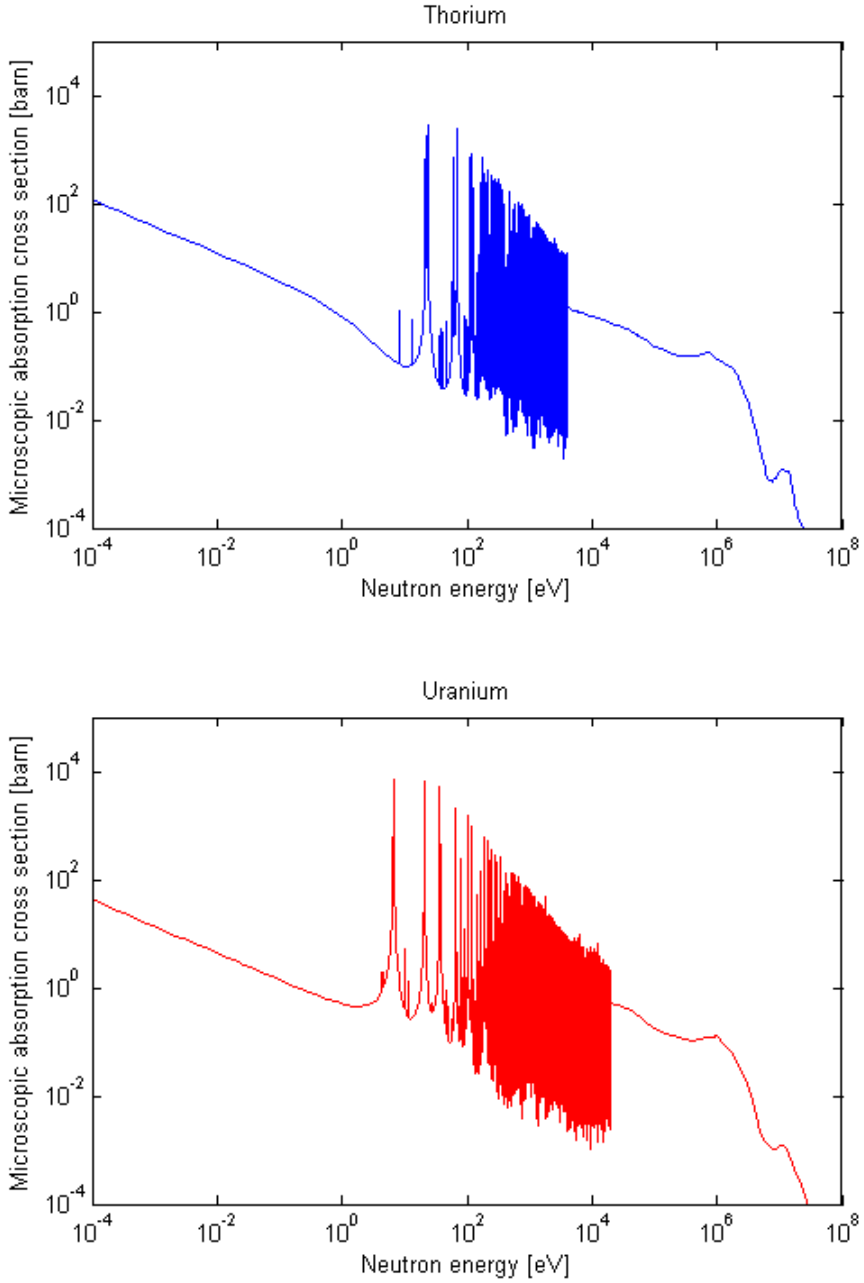

Figure 2.1: The capture cross section for ^{232}Th and ^{238}U [10].

2.2.3 Uranium

^{233}U produced from thorium is a potent fissile element as it gives a better neutron economy than with ^{235}U and ^{239}Pu. The capture and fission cross sections for thermal neutrons are 47 barn and 530 barn respectively, giving a capture to fission ratio of 0.093, compared to 0.175 for ^{239}Pu and 0.370 for ^{235}U [11]. The number of emitted neutrons per absorbed thermal neutron in the fuel is also higher for ^{233}U than for ^{235}U and ^{239}Pu, 2.30 compared to 2.11 and 2.15 [12]. Fission of ^{233}U releases about the same energy as that of ^{235}U, ~ 200 MeV. When ^{233}U captures a neutron, it transmutes into ^{234}U, which is an unwanted neutron absorber [9].

2.3 Self-shielding

Self-shielding is an important aspect to consider in systems containing much fertile and fissile material. It expresses itself as giving a lower neutron flux in the middle of the fuel pin compared to the rim. There are two major reasons for this; capture of thermal and epithermal neutrons [13]. Because no thermal neutrons are created in the fuel pin, they can only enter the pin from the outside, and as the neutrons travel inwards some are captured and thus the thermal flux is decreased. The epithermal neutrons will be absorbed by the large resonance capture regions of certain fissile and fertile isotopes. This will lead to a reduction of the flux in the center as well as a build up of fissile isotopes at the rim, further increasing the effect of the thermal neutrons.

Isotopes with a high resonance capture are ^{238}U and ^{232}Th. ^{239}Pu also has resonance peaks in the epithermal energy region which are considered non-negligible. Th-MOX fuel will have a larger self-shielding of thermal neutrons but a smaller self-shielding of epithermal neutrons because of the higher overall capture cross section but a smaller resonance region, as described in Section 2.2.1 and 2.2.2.

The consequence of this in the environment of a fuel pin is that the build up of fissile ^{233}U in the rim will be relatively less compared to build up of ^{239}Pu, but the overall build up in the pin will be higher, see Figure 2.2. By reducing the amount of fissile build up in the rim of the pin, the power profile will be affected as well. The relative power at the rim will not increase at high burnup, resulting in a flatter power profile.

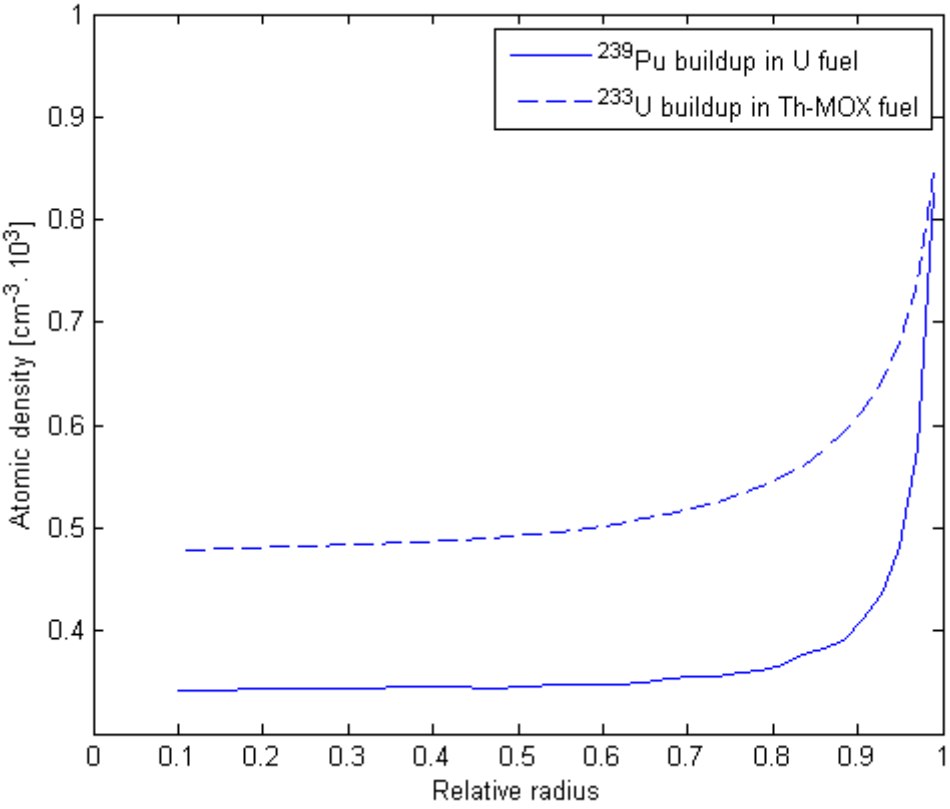

Figure 2.2: The build up of fissile elements in U and Th-MOX fuel after a burnup of 70 $\frac{GWd}{tHM}$. The fertile content of heavy metal in both fuels is slightly over 92 % to give a fair comparison.

In a heavy water reactor where there is more moderator, a larger fraction of the neutrons are in the thermal part of the spectrum so there will not be as many epithermal neutrons. This will lead to more shelf shielding by thermal neutrons and less by epithermal, reducing the rim effects even further.

2.4 FRAPCON's procedure

Both the old TUBRNP model proposed by K. Lassmann [14] and the new model developed called Total Thorium Plutonium BuRNup (TTPBRN) calculate the radial power profile in three separate steps, explained in the following sections:

1. Calculate local atomic densities
2. Approximate neutron flux

3. Use the concentrations and flux to calculate power profile

The TUBRNP method proved to be inaccurate in describing the radial power profile for Th-MOX fuel. This is because of the larger absorption cross section of thorium and plutonium, which violates the underlying assumptions in Fick's law and thereby the diffusion approximation and probably also because of resonances in the fission cross section for ^{239}Pu. Fick's law is only valid if the macroscopic absorption cross section is less than the macroscopic scattering cross section $\Sigma_a \ll \Sigma_s$ [15].

The major differences between these two models are the set of isotopes, the implementation of the shape function, explained in Section 2.4.1 and the calculation method of the neutron flux.

The physical properties considered in the models are the dimensions of the pellet, the atomic densities of the fuel, the different cross sections of the fuel, density of the fuel and the porosity of the fuel. What is not a part of the model is related to the properties of the moderator, including the temperature and density/void of the moderator, properties of the cladding, cladding gap and the distribution of the fuel pins in the reactor.

FRAPCON uses effective cross sections for all calculations. These are empirically obtained, which compensates for the properties not included in the model. For example the neutron spectrum, moderator properties and cladding. They are adapted to reproduce the power profiles found experimentally or by simulations with sophisticated neutronic software, and are not necessarily closely related to the experimentally determined neutron reaction cross sections found in cross section libraries.

2.4.1 Calculation of local atomic densities

The fuel pin in the model is divided into several annular nodes, defined by user input or by FRAPCON if no user input is provided. A set of differential equations, called the Bateman equations, describe the average concentration of isotopes in the fuel.

$$\frac{d\bar{N}_j}{dt} = -\sigma_{a,j}\bar{N}_j\phi + \sigma_{c,j-1}\bar{N}_{j-1}\phi \tag{2.1}$$

Here $\bar{N}$ is the average atomic concentration, σ_a is the microscopic absorption cross section, σ_c is the microscopic capture cross section and j is the isotopes present in the model. As input, FRAPCON takes a set of discrete burnup intervals, and solves the system one step at a time. Therefore these equations are discretized by approximating $\frac{d\bar{N}}{dt}$ as $\frac{\Delta\bar{N}}{\Delta t}$

Instead of writing the increment as a function of the fluence $\Delta t\phi$ it is more convenient to express it as a function of the burnup Δbu. This is performed using the conversion

$$\Delta bu = \frac{q'''\Delta t}{\rho_{fuel}} = \frac{\alpha}{\rho_{fuel}}\sum_k \sigma_{f,k}\bar{N}_k\phi\Delta t \tag{2.2}$$

where σ_f is the microscopic fission cross section, q''' the volumetric heat generation rate, ρ_{fuel} the density of the fuel and α a unit conversion coefficient. The discretized time

derivate is rewritten using

$$\frac{\Delta t\phi}{\Delta bu} = 0.8815\frac{\rho_{fuel}}{\alpha\sum_k \sigma_{f,k}\bar{N}_k} \equiv A \tag{2.3}$$

and multiplied with Equations 2.1. Instead of using the average concentration, the dependence on the radial position is introduced. The resulting and final equations are as follows:

$$\frac{\Delta N_j(r)}{\Delta bu} = -\sigma_{a,j}N_j(r)A + \sigma_{c,j-1}N_{j-1}(r)A \tag{2.4}$$

These atomic densities are evaluated for each radial node of the pin using the local atomic densities. The full description of the Bateman equations is found in Section 2.4.1.

The TUBRNP method

The set of Bateman equations used in the TUBRNP method is:

$$\frac{\Delta N_{U235}(r)}{\Delta bu} = -\sigma_{a,U235}N_{U235}(r)A \tag{2.5}$$

$$\frac{\Delta N_{U238}}{\Delta bu} = -\sigma_{a,U238}\bar{N}_{U238}f(r)A \tag{2.6}$$

$$\frac{\Delta N_{Pu239}(r)}{\Delta bu} = -\sigma_{a,Pu239}N_{Pu239}A + \sigma_{c,U238}\bar{N}_{U238}f(r)A \tag{2.7}$$

$$\frac{\Delta N_j(r)}{\Delta bu} = -\sigma_{a,j}N_j(r)A + \sigma_{c,j-1}N_{j-1}(r)A \tag{2.8}$$

Here j represents the Pu isotopes 240, 241 and 242. For ^{238}U the average atomic density $\bar{N}_{U238}$ is still used and is multiplied with a shape function $f(r)$. This shape function takes care of the uneven production of fissile plutonium due to self-shielding because of resonance capture of epithermal neutrons, see Section 2.3. The shape function has the form:

$$f(r) = 1 + p_1 e^{-p_2(R_0-r)^{p_3}} \tag{2.9}$$

Where p_1, p_2 and p_3 are three empirically predetermined parameters and R_0 is the outer radius of the pin. $f(r)$ is normalized to have the volume averaged value of 1 by a normalization factor defined as follows:

$$\frac{\int_\theta \int_{R_I}^{R_0} f(r) r dr d\theta}{\int_\theta \int_{R_I}^{R_0} r dr d\theta} = 2\frac{\int_{R_I}^{R_0} f(r) r dr}{R_0^2 - R_I^2} \tag{2.10}$$

R_I is the inner radius and is 0 in case of a solid fuel pellet. This shape function has not been derived from any physical phenomena, and is only used because it has been found to describe very well the uneven capture rate due to epithermal neutrons.

The TTPBRN method

This model is similar to the one proposed by Y.Long [16], where Th-U fuel is modeled, with the exception of the changed shape function. The new isotopes in this model are ^{232}Th, ^{233}U, ^{234}U, ^{236}U and ^{238}Pu, each one with a unique set of cross sections and corresponding Bateman equations. The new set of terms in the Bateman equations for the calculation of the atomic densities are the following:

$$\frac{\Delta N_{Th232}(r)}{\Delta bu} = -\sigma_{a,Th232}(r)N_{Th232}(r)A(r) \tag{2.11}$$

$$\frac{\Delta N_{U233}(r)}{\Delta bu} = \sigma_{c,U232}(r)N_{U232}(r)A - \sigma_{a,U233}(r)N_{U233}(r)A(r) \tag{2.12}$$

$$\frac{\Delta N_{Pu238}(r)}{\Delta bu} = -\sigma_{a,Pu238}N_{Pu238}(r)A(r) \tag{2.13}$$

$$\frac{\Delta N_{j}(r)}{\Delta bu} = \sigma_{c,j-1}N_{j-1}(r)A(r) - \sigma_{a,j}N_{j}(r)A(r) \tag{2.14}$$

Here j is the isotopes ^{234}U, ^{235}U, ^{236}U, ^{239}Pu, ^{240}Pu, ^{241}Pu and ^{242}Pu.

It is worth noticing that the cross sections of ^{232}Th and ^{239}Pu are dependent on the radial position in the pin, see Equation 2.15.

$$\sigma_{c,Th232}(r) = \bar{\sigma}_{c,Th232} \cdot f_{Th232}(r) \tag{2.15a}$$

$$\sigma_{f,Pu239}(r) = \bar{\sigma}_{f,Pu239} \cdot f_{Pu239}(r) \tag{2.15b}$$

A shape function, $f(r)$, is applied to the capture cross section of ^{232}Th and fission cross seciton of ^{239}Pu instead of applying it to the build up directly as in the TUBRNP model. This allows the neutron flux, and thereby the power profile to be directly dependent on radial variations of isotopic concentrations in the fuel because of the capture of epithermal neutrons. The form of the shape function is similar to the one in the TUBRNP model with the exception that the coefficients are dependent on the atomic density of ^{239}Pu and the radius of the fuel pin, see Equation 2.16.

$$f_{Th232}(r) = 1 + C_1(R_0) \cdot e^{C_2 \cdot (R_0 - r)^{C_3}} \tag{2.16a}$$

$$f_{Pu239}(r) = 1 + D_1(R_0, N_{Pu239}) \cdot e^{D_2(N_{Pu239}) \cdot (R_0 - r)^{D_3(N_{Pu239})}} \tag{2.16b}$$

The coefficients differ between heavy and light water conditions. Both shape functions are normalized to 1. These coefficients cannot be determined analytically and have to be found empirically the same way as the effective cross sections. The coefficients have been altered compared to the old model by adding a dependence on the ^{239}Pu concentration and outer radius. This is purely empirical and is only performed because it describes the system better.

^{233}Th and ^{233}Pa are two intermediate isotopes in the formation of ^{233}U which have very large absorption cross sections and a very short half-life. Because of the change

from Δt to Δbu in the model the dependence on only time for the half-life is problematic. The fraction p of ^{233}Th and ^{233}Pa consumed by decay can be expressed as:

$$p = \frac{\lambda}{\lambda + \sigma_a \phi} \tag{2.17}$$

Considering the total absorption cross section of 1500 barn for ^{233}Th and 39 barn [8] for ^{233}Pa, the half-lives of 22.3 minutes for ^{233}Th and 27.0 days for ^{233}Pa and a flux of about $10^{13}\ \frac{n}{cm^2}$ which is normal for a LWR, the percentage of decay exceeds 99 %. This means that the fraction of neutrons captured can be neglected, so ^{233}Pa and ^{233}Th can be assumed to decay instantaneously.

2.4.2 Approximation of neutron flux

The power profile in a fuel pin is described by the fission cross section, the atomic density and the neutron flux. A simple model for acquiring this neutron flux is thus needed. The neutron flux is described accurately by the transport equation, which for steady state problems reads:

$$\begin{aligned} &\bar{\Omega} \cdot \bar{\nabla}\psi\left(\mathbf{r}, \bar{\Omega}, E\right) + \Sigma_T\left(\mathbf{r}, E\right)\psi\left(\mathbf{r}, \bar{\Omega}, E\right) \\ &= \textstyle\int_{4\pi}\int_0^\infty \Sigma_S\left(\mathbf{r}, \bar{\Omega}' \to \bar{\Omega}, E' \to E\right)\psi\left(\mathbf{r}, \bar{\Omega}', E'\right)\, d\omega' dE' \\ &+ \tfrac{\chi(E)}{4\pi}\textstyle\int_0^\infty \nu\Sigma_f\left(\mathbf{r}, E'\right)\phi\left(\mathbf{r}, E'\right)\, dE' \end{aligned} \tag{2.18}$$

ϕ is the scalar neutron flux, ψ the angular neutron flux, $\bar{\Omega}$ the direction, E the energy, $\chi(E)$ the prompt neutron spectrum, ν the average number of neutrons emitted by fission, $\mathbf{r}$ the position, Σ_T the total macroscopic cross section, Σ_S the macroscopic scattering cross section and Σ_f the macroscopic fission cross section [15].

This is a very tricky equation to solve because of its multidimensional properties. Both the position $\mathbf{r}$ and the direction of the neutrons $\bar{\Omega}$ are two dimensional and together with the energy, E, this gives a six dimensional problem. A common simplification of this problem is the so called diffusion approximation, which for some cases can be solved analytically. The approximations made during the derivation of the diffusion approximation are listed below:

- Infinite homogeneous medium
- No neutron source
- Flux varying slowly with position
- Isotropic scattering in the laboratory system
- Steady-state conditions

Fick's law is expressed as:

$$\mathbf{J}(\mathbf{r}, E) = -D(\mathbf{r}, E)\bar{\nabla}\phi(\mathbf{r}, E), \tag{2.19}$$

where $\mathbf{J}$ is the neutron current density vector, defined as the mean flux in a specific direction, and $D(\mathbf{r}, E)$ is the spatial and energy dependent diffusion coefficient, [15]. One of the conditions under which Fick's law is valid concerns the cross sections of the fuel. This is that the macroscopic absorption cross section must be much smaller than the macroscopic scattering cross section, $\Sigma_a \ll \Sigma_s$ [15].

The multi group diffusion equation can be written as:

$$\bar{\nabla} \cdot \left(-D_g\left(\mathbf{r}\right)\bar{\nabla}\phi(\mathbf{r})\right) + \Sigma_{T,g}(\mathbf{r})\phi_g(\mathbf{r}) = \sum_{g'=1}^{G} \Sigma_{s0,g'\to g}(\mathbf{r})\phi_{g'}(\mathbf{r}) + \frac{\chi_g}{k}\sum_{g'=1}^{G} \nu_{g'}\Sigma_{f,g'}(\mathbf{r})\phi_{g'}(\mathbf{r}) \tag{2.20}$$

$D_g(\mathbf{r})$ is the group and spatially dependent diffusion coefficient and G is the number of energy groups. Rewriting Equation 2.20 with the simplification of a one group system and the assumptions of a homogeneous fuel, rotational invariance, only thermal neutrons interact with the fuel, no production of thermal neutrons in the fuel and writing the equation in cylindrical coordinates, one ends up with the following expression

$$\frac{d^2\phi}{dr^2} + \frac{1}{r}\frac{d\phi}{dr} - k_f^2\phi = 0 \tag{2.21}$$

where $k_f^2 = \frac{\Sigma_a}{D}$, [13]. Together with the boundary conditions of continuity of the flux at the boundary and continuity of its space derivative in the center:

$$\phi(r)|_{r=R_0} = \phi_0 \tag{2.22}$$

$$\left.\frac{d\phi(r)}{dr}\right|_{r=R_I} = 0 \tag{2.23}$$

the system can easily be solved, [13].

The TUBRNP model

The old TUBRNP model uses an analytical approach to Equation 2.21. k_f is assumed to be constant in the fuel pin, which leads to solutions in the form of a Bessel function, or a combination of Bessel functions.

$$\phi(r) \propto I_0\left(k_f r\right) \tag{2.24}$$

$$\phi(r) \propto I_0\left(k_f r\right) + \frac{I_1\left(k_f R_I\right)}{K_1\left(k_f R_I\right)} \cdot K_0\left(k_f r\right) \tag{2.25}$$

Equation 2.24 is valid for non hollow and 2.25 is the solution for hollow pins. I and K are modified Bessel functions of first and second kind respectively and the subscripts are the order. Since k_f is constant, the neutron flux cannot be dependent on the radial composition of the fuel.

The TTPBRN model

In the TTPBRN model the neutron flux is solved numerically using a finite difference method. This allows for calculation of the neutron flux in a pellet with radially varying cross sections and isotope concentration, which is the case after irradiation and specially with the new adaption of the shape function.

A cartesian geometry is used, instead of a polar geometry, for the finite difference method. This is because the equations become much simpler. The errors introduced are corrected for later on and are therefore very small. Equation 2.20 is used, where the diffusion term is approximated as:

$$\frac{J_{n+1} - J_n}{\Delta r} \tag{2.26}$$

obtained by integrating around the radial node n. J is also approximated using Fick's law, Equation 2.19, resulting in the final form

$$a_n\phi_n + b_n\phi_{n+1} + c_n\phi_{n-1} + \Sigma_{a,n}\phi_n = 0 \tag{2.27}$$

where

$$c_n = -\frac{D}{\Delta r_n \cdot \Delta r_{n-1}} \tag{2.28a}$$

$$a_n = \frac{D}{\Delta r_n \cdot \Delta r_{n-1}} + \frac{D}{\Delta r_n^2} \tag{2.28b}$$

$$b_n = -\frac{D}{\Delta r_n^2} \tag{2.28c}$$

This equation works for all nodes except the end nodes where equations are derived assuming $J_0 = 0$ and $\phi_n = Const.$ These terms can be arranged into a matrix, containing values on the diagonal and on the subdiagonal and superdiagonal, forming a so called tridiagonal matrix, see Figure 2.3. The problem can thus be described by a matrix equation:

$$\mathbf{A}\bar{\phi} = \bar{b} \tag{2.29}$$

where $\mathbf{A}$ contains the diffusion and absorption term and $\bar{b}$ contains only one constant from the last node, that describes the amount of neutrons entering the system. This equation is easily solved using existing methods for tridiagonal matrices, in this case a subroutine in Lapack, which is a software library written in Fortran 90 for numerical linear algebra [17].

$$\begin{pmatrix} a_1 & b_1 & & & 0 \\ c_1 & a_2 & b_2 & & \\ & c_2 & a_3 & \ddots & \\ & & \ddots & \ddots & b_{n-1} \\ 0 & & & c_{n-1} & a_n \end{pmatrix}$$

Figure 2.3: The shape of the tridiagonal matrix A.

2.4.3 Calculation of power profile

The volumetric power generation, and with it the power profile, is calculated by:

$$q''' \propto \sum_j \sigma_{f,j} N_j \phi \tag{2.30}$$

and uses the effective cross sections. They can only be, and have been, acquired empirically. FRAPCON uses this procedure and normalizes the power to unity with Equation 2.10. The cross sections and atomic densities are only used internally in the subroutine, while the normalized power profile is used by some external subroutines.

2.5 Genetic Algorithm

To solve a problem with a large set of unknown parameters/variables a Genetic Algorithm (GA) [18] can be employed. This is a biologically inspired method where a population of chromosomes competes to replicate themselves. A chromosome better adapted to the problem has a higher chance of surviving and spread its genes. It is a method of finding an optimum of an function $f(x_1, ..., x_n)$, called the objective function, of n variables in the search space $\mathbf{x} = (x_1, ..., x_n)$. Variables, $\mathbf{x_k}$, in this search space are encoded into a vector of numbers, called a chromosome, with either binary or real value encoding. These binary or real values are called the genes. A GA is an iterative method where each step is called a generation, and the individuals are replaced between each step.

Each step in the procedure of finding an optimum of the objective function is listed below, and the items in the list are described in more detail in the following sub sections.

1. Initialization
2. Evaluation
3. Selection
4. Crossover
5. Mutation

6. Replacement
7. Elitism

2.5.1 Initialization

This step is done only once, before the iterative process begins. A set of initial chromosomes is generated, the first generation population. Chromosomes are either randomly selected from the entire search space or according to some predetermined pattern and rules. In this case the population was sampled around an initial guess relatively close to the assumed optimum, using a real value encoding.

2.5.2 Evaluation

In the evaluation step each chromosome is interpreted and fit into the objective function. Here the values in the chromosome are used as cross sections and shape function parameters directly.

These values are used to evaluate the objective function for the problem, which is the new subroutine TTPBRN. From the evaluation or from postprocessing of the data from the evaluation, a fitness value is assigned to each chromosome which is a representation of how well the chromosome solves the problem, where a higher fitness represents a better solution. The fitness value in this case is the sum of square error of the output and precalculated data, see Section 2.6. The sum of square can be calculated using the following equation

$$\epsilon = \frac{\sum_{i=1}^{N} (x_i - y_i)^2}{N} \tag{2.31}$$

Here y are the data simulated by Serpent, x are values calculated by the FRAPCON model and N is the total number of nodes. N represents here all radial and burn up nodes of a fuel pin calculation.

2.5.3 Selection

A new population is selected from the old guided by the fitness values previously calculated. Chromosomes are chosen, two at a time with a selection algorithm called tournament selection. In this variant of tournament selection two individuals are randomly chosen from the population. A random number is generated between 0 and 1 and if this random number is below a threshold, the tournament selection parameter, (always above 0.5), the individual with the highest fitness is selected.

2.5.4 Crossover

For every two new individuals crossover is performed with a certain probability. This means that if a random value between 0 and 1 falls under a threshold provided by the user, the crossover probability, a random point is chosen between the genes where

the chromosome is cut and switched between the two individuals, see Figure 2.4. This operation ensures that the new population most likely will have a better fitness than the previous, given that the crossover provided the best genes from both old chromosomes to the two new ones.

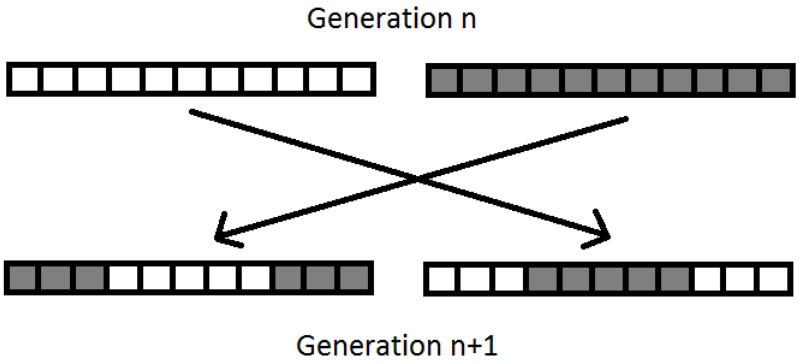

Figure 2.4: Schematic representation of the crossover process.

2.5.5 Mutation

All new chromosomes created will be subject to mutations. All genes in every chromosome are assigned a random number between 0 and 1. If it falls below a threshold selected by the user, the mutation probability which is usually set to $1/n$, where n is the number of genes, a mutation will occur. For real value encoding the most common way to implement mutation is to define a creep rate, r. The mutation changes the value of the gene by a random number in the interval [-r, r] either linearly or according to a distribution. This operation is a way to maintain diversity in the population, and prevent the population to get stuck in local optima.

2.5.6 Replacement and Elitism

To eliminate the risk of the best individual in a simulation to be lost due to random chance, a final step called elitism is implemented. What it does is taking the best individual in the previous population and inserting it into the new, without the need of going through the steps of selection, crossover and mutation. Because of this the maximum fitness will always be an increasing quantity. The old population is then finally replaced by the newly created one and the process is repeated.

2.5.7 Application of a GA

Using a classical optimization method with an extensive amount of variables can be very complicated, especially when the problem is highly non-linear. A stochastic approach like a GA on the other hand is an easy method to implement, and can quite easily find

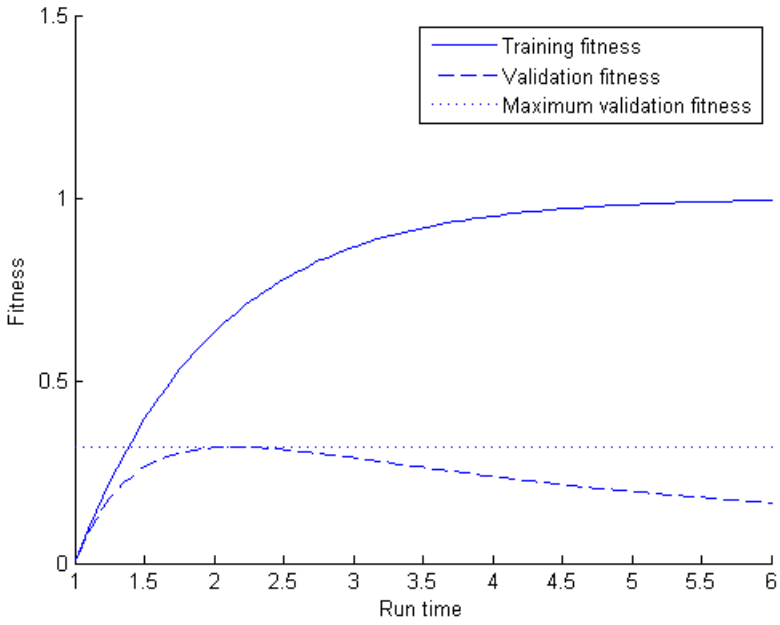

Figure 2.5: A representation of the behaviour for the training and validation fitness.

good solutions to complex problems. It does not always find the best solution due to its stochastic nature, but if a good solution exists it will most likely be found.

2.5.8 Experiment design

Often only a limited amount of data can be collected for the parameter determination due to time or economical constraints. With a small amount of data a problem called overfitting may occur. This arises because the algorithm fits the parameters very specifically to the data points given and not to the problem as a whole. To accommodate for this shortcoming the set of cases is divided into two subsets, the training set and the validation set. While the training set provides the feed-back to the genetic algorithm the validation set does not. It is simply evaluated each generation to determine how generally the parameters solve the problem. Because the training set provides feedback, the fitness of this set will always increase. For the validation set, the fitness value will increase as long as the GA provides a better solution to the general problem and decrease when the GA starts to solve the specific cases instead. When this happens the GA is stopped and the population with the best fitness with respect to the validation set will be used. This is illustrated in Figure 2.5.

2.6 Monte Carlo simulation

Monte Carlo (MC) is a method of solving numerical problems by random sampling. The basic idea is to formulate a stochastic model of the problem at hand, sample data from an appropriate distribution and then estimate the answer with the use of statistical methods. One could for example estimate physical constants, for example π or numerical integrals by sampling with a flat distribution on a 2d plane. Figure 2.6 shows a simulation with 30 points randomly distributed within a square of side R. The points inside the circlewhich has the diameter R are defined by, $x^2 - y^2 < R^2$ and the ratio $\frac{A_{Circle}}{A_{Square}} = \frac{\pi}{4}$. One can thus estimate π by counting the number of points inside the circle and multiply it by 4. A similar method can be used for particle simulation, where the initial particle is created with properties randomly sampled with appropriate distributions. This particle could be a neutron where the variable estimated is the number of prompt neutrons per absorbed slow neutron, or the number of neutrons absorbed in a certain material.

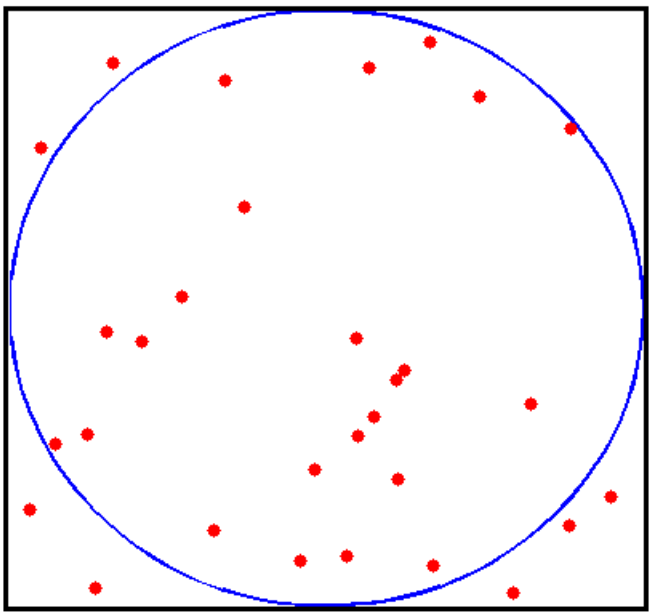

Figure 2.6: Points sampled with a flat distribution in a 2D plane.

2.6.1 Statistical properties

There are three main requirements for the MC method [19]. Firstly a set of random numbers needs to be generated. Secondly the problem at hand must be described stochastically, where the history of a particle can be simulated by statistical data and analytical methods. Such examples are emitted particle distributions and reaction laws from ENDF data, see Section 2.6.2. Lastly the problem needs to have a Markovian property, i.e. the simulations only depend on the current state and not the previous simulations.

If the requirements are fulfilled for the problem, the law of large numbers can be

applied [20]. It states that as the number of samples goes to infinity, the mean value will approach the expected value.

$$E[x] = \lim_{N\to\infty} \frac{1}{N} \sum_{i=1}^{N} x_i \tag{2.32}$$

Here x is the property obtained in the simulation and N is the number of samples. The central limit theorem can also be applied which states [21] that with an increasing number of data points the calculated value of the mean/expected value will be distributed according to a normal distribution. This can be used to estimate the uncertainty, as the variance of a normally distributed variable is proportional to $\frac{1}{\sqrt{N}}$.

2.6.2 Particle simulation

In MC simulations particle transport is handled by releasing particles into the geometry in question, and following their path. The histories of all particles is used to get a mean value of the property in question. The particles are sampled with a random speed and direction and in interactions with the material, new properties are sampled with regards to the nature of the particle and interaction. For neutrons the interactions might be elastic collisions, inelastic collisions, capture or fission reactions [19]. Often the resonance regions in fertile materials are treated using probability table sampling, where instead of using cross section data with too low resolution to fully resolve the resonances, a probability distribution is applied, [22]. This is applied in the Serpent code [4].

2.6.3 Model

When considering particle simulation there are some requirements for the model. Composition, temperature and densities of the materials in the model need to be specified as well as the geometry of the object, the boundary and boundary conditions. If neutrons are simulated in a criticality calculation cross sections and fission yields are also required.

2.6.4 Approach by Serpent

This section is partly based on the Serpent manual [4]. Serpent performs a k-eigenvalue criticality calculation. It releases neutrons into the geometry and follows their history, repeating it for several cycles. The spatial, energy and angular distribution of the neutrons in each cycle comes from the distribution of fission reactions in the previous cycle, and the first cycle uses a source randomly distributed in the fissile cells of the geometry. Each cycle has a fixed number of neutrons, selected by the user. For each cycle a k-value and other properties selected by the user are calculated. The value for all cycles are combined to give the expected value, Equation 2.32, along with the uncertainty. Some of the first cycles are discarded from the statistics. This is to allow the distribution of the neutrons to get into steady state, due to the randomly distributed source in the first cycle.

Serpent can also run in an external source mode, where a source and a spectrum is defined by the user. This is useful when the system is sub-critical, for example during irradiation of test rods inside a critical reactor. The procedure for this mode is the same as for the k-eigenvalue criticality mode, in that it simulates several cycles where the first are discarded. The expected value and the uncertainty are then calculated from all the cycles.

2.6.5 Advantages and disadvantages

There are many advantages with the MC methods compared to other numerical methods. It is often very simple to set up the computational model. Because MC is a stochastic model, there is no need to know anything about the analytical solutions to the problem. Neither is there need for the many simplifications often seen in deterministic codes, for example energy groups and resonance integrals. These simplifications are often based on uranium fuel and will not necessarily be optimal for Th-MOX fuel. There is also no need to do any simplifications in the geometry of the model. All these things contribute to a more exact representation of the problem, contrary to deterministic models.

In contrast to the advantages of this method there are also some negative sides. One major disadvantage is the CPU intensity, which is very high and limits the usefulness of MC simulations in many applications. This is not a big obstacle in this work since the model is very simple, which makes MC a very useful method.

3

METHODS

3.1 Working procedure

Initially a sensitivity analysis on the power profile was performed regarding the physical properties not included in the FRAPCON model. Afterwards the reference cases were simulated using a variety of pin configurations. Both these steps were done using the same pin model simulated in Serpent. With the reference cases the genetic algorithm found the optimal set of cross sections and shape function parameters for the problem, which was implemented in FRAPCON. The genetic algorithm was implemented using MatLab. The new model was analysed using various statistical concepts. Cross sections and shape function parameters were found for both LWR and the Halden Boiling Water Reactor (HBWR).

3.2 Sensitivity analysis

The purpose of the sensitivity analysis was to assess whether or not some physical properties and parameters in the reactor that were not included in the FRAPCON procedure/subroutine were important for the shape of the power profile. These parameters were the:

- Void fraction in moderator
- Average fuel temperature
- Pin pitch
- Linear heat generation rate

A low sensitivity of a parameter meant it was safe to exclude the perturbation of it in the generation of the reference cases.

One standard case was created, along with several other sensitivity cases where one parameter was modified up and down. These sensitivity cases where compared to the standard case and evaluated. The modified variables and the magnitude of the modification are shown in Table 3.1.

Table 3.1: Parameters for reference case and the range of modification for the sensitivity analysis.

Parameters	Reference case	Perturbed cases
Void fraction in moderator [%]	40	0, 70
Average fuel temperature [^{o}C]	800	400, 1200
Pin pitch [cm]	1.295	1.0, 2.0
Linear heat generation [$\frac{W}{cm}$]	30	10, 60

3.2.1 Results of sensitivity analysis

The sensitivity analysis showed that the average fuel temperature and the linear heat generation rate had very little impact on the final profile, see Figure 3.1, and hence they were not considered when creating the reference cases and was set to a representative value. The void fraction and pin pitch on the other hand had a large impact, see Figure 3.2. The other plots of sensitivity cases can be found in Appendix B.

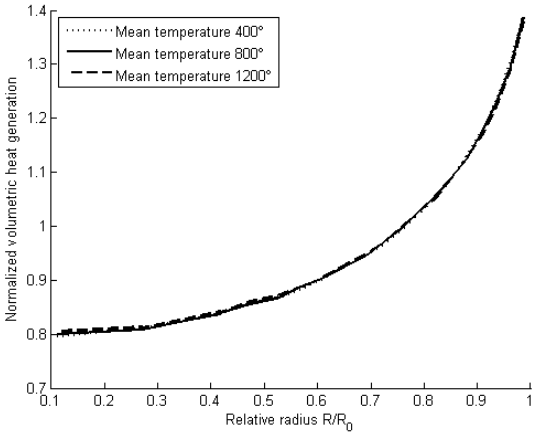

Figure 3.1: The sensitivity for the temperature in the fuel pin.

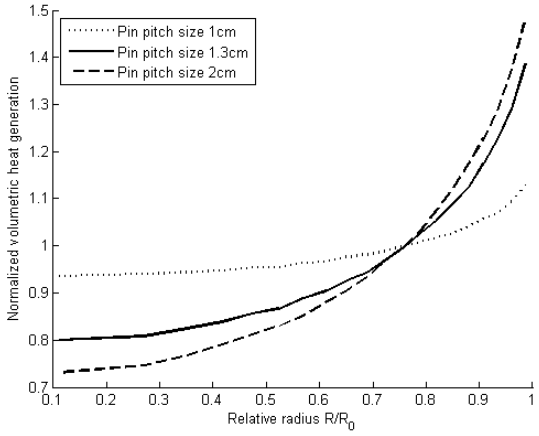

Figure 3.2: The sensitivity for the fuel pin pitch.

3.2.2 Discussion of the sensitivity analysis

The effect of the radial power profile by perturbation of the linear heat generation and the fuel temperature was small. This is not surprising because a homogeneous change in the whole pin ought to change the power homogeneously everywhere, and thus nothing really changes in the power profile. More is expected to change when the temperature is changed inhomogeneously, with a higher temperature in the middle, as this will change the effect of the Doppler broadening. The feedback from the thermomechanical calculations to the neutronic simulations required to model this effect is however not implemented in the current FRAPCON version, and introduction of such feedback is outside the scope of this thesis work.

The sensitivity analysis showed that the ratio of the fuel and moderator, the hydrogen to heavy metal ratio (H/HM) ratio, tested with different void fraction and pin pitch size, had a large impact on the power profile. This effect is attributed to the ratio between the fast and thermal neutron spectra. A larger amount of moderator compared to fuel gives more moderation and a larger fraction of the neutrons fall within the thermal spectrum and vice versa. The radial profile for the thermal and fast flux is shown in Figure 3.3. Most of the fission reactions come from thermal neutrons, and when most neutrons are thermal, it is the dominating contributor to the shape of the flux. When the fast neutron fraction becomes very high, it starts to influence the power profile, making it more flat as the fast flux is larger in the center instead of at the rim as with the thermal flux. This effect was neither considered in the FRAPCON code nor in the new THUPS model for Th-U fuel developed by Yun Long [16]. Most configurations of reactors [23] have a similar value for the H/HM ratio, and consequently one representative value was chosen for both the BWR and PWR cases and no distinction was made between them. H/HM for BWR were 2.0 - 2.4 and for PWR 2.3 - 2.7. There were some cases that were outside these limits though. The value for the reference cases was chosen to around 2.2.

There were some reasons why this was not considered in the new TTPBRN model.

As described in [13], to fully consider this effect, one would need either a full description of the neutron flux with many energy groups, or knowledge of the amount of neutrons in each group. Solving a diffusion problem with several energy groups would require a lot more computational power and probably the use of more empirical and simulated physical parameters. The code would be dependent on more external codes like Lapack. Neither of this is good since the subroutine will be executed many times, several hundred times for the calculation of one case.

All sensitivity cases were simulated using LWR conditions. The results for linear heat generation rate and average fuel temperature were assumed also to be valid for HBWR cases and no further sensitivity analysis was performed. A different method was used for the creation of the HBWR cases, described in Section 3.3.1 which rendered the pin pitch size and void fraction insignificant.

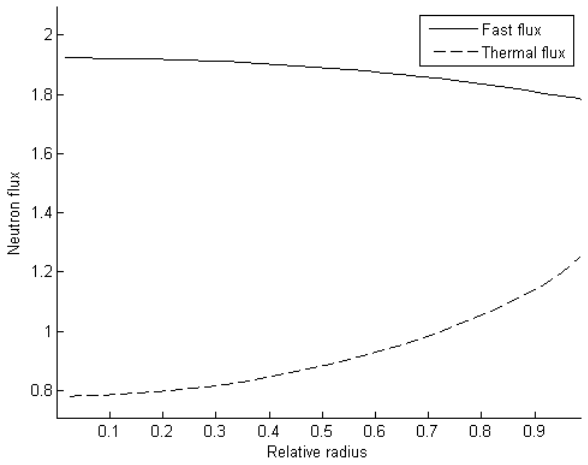

Figure 3.3: The shapes of the thermal and fast flux. The magnitudes of the fluxes are not in scale.

3.3 Reference data generation

A simple model of the fuel pin was created and simulated in Serpent for the purpose of finding the radial power profile.

3.3.1 Pin model

In the LWR case the system consisted of a single fuel pin bounded by a cube. A cubical shape fulfills the conditions for 8-fold symmetry, which was applied, together with reflective boundary conditions. This simulated an infinite lattice of fuel pins.

The pin consisted of three or four parts, depending on the case. Outermost was the cladding of Zircalloy material with a thickness of about 0.65 mm and a temperature of

327 °C. Inside of this was the cladding gap, a space of about 0.17 mm filled with air of 800 °C. Next was the fuel pellet, which in some cases was hollow and filled with air.

The exterior of the pin consisted of moderator liquid, either heavy or light water with a density corrected by the void fraction. The fuel in the pin was divided into several annular depletion zones of equal volume and a detector was added to each to acquire the total power deposition. The fuel temperature was 800 °C and the linear heat generation rate, q' was 30 $\frac{W}{cm}$.

The pin pitch was chosen so that the total volume consisted of 33 % fuel, excluding the hole present in some of the pins, this gave a H/HM ratio of about 2.2. The temperature of the fuel and the air in the hollow pins was homogeneous at 800 °C. The density and temperature of the moderator were set to saturated conditions at 70 bar, which were 0.739 $\frac{g}{cm^3}$ (excluding void) and 285 °C respectively.

Each fuel pellet was divided into 25 radial zones of equal volume where all properties were averaged. The power output in each zone was obtained via simulated detectors placed in each zone.

To allow for adequate accuracy in the calculations but still reasonably short calculation time in the LWR case, each step consisted of 30 discarded and 500 used cycles with 9000 particles in each. This gave a calculation time of 8 h and a relative error for the power in each zone of about 0.3 %.

The HBWR system was modeled a bit differently to get the right neutron spectrum in the Th-MOX fuel to simulate the conditions in the Halden research reactor, which was used for validation purposes. This was done by inserting the Th-MOX pin in the middle of a 3 by 3 lattice consisting of normal uranium pins. The pin pitch was adjusted so that the neutron spectrum in the cladding for the thorium pin was consistent with a typical spectra provided by the operators of the the Halden reactor [24]. More moderator is needed to thermalize neutrons when using heavy water because of the heavier nuclei. Thus the pin pitch was larger than for the LWR model, 6.4 cm. The pin pitch was also kept constant for all cases not to disturb the spectra. Some small changes in the spectrum were introduced by the varying thorium pin, but it was smaller than the uncertainty in the reference spectra. The reference spectra from Halden and the final spectra in the modeled fuel can be seen in Figure 3.4. Only 5000 particles were simulated for each cycle to reduce the calculation time due to the more complex problem, which gave a calculation time of around 7 h, but a larger relative error in the simulation, which was about 0.8 %. All other parameters for the HBWR cases were the same as for the LWR cases.

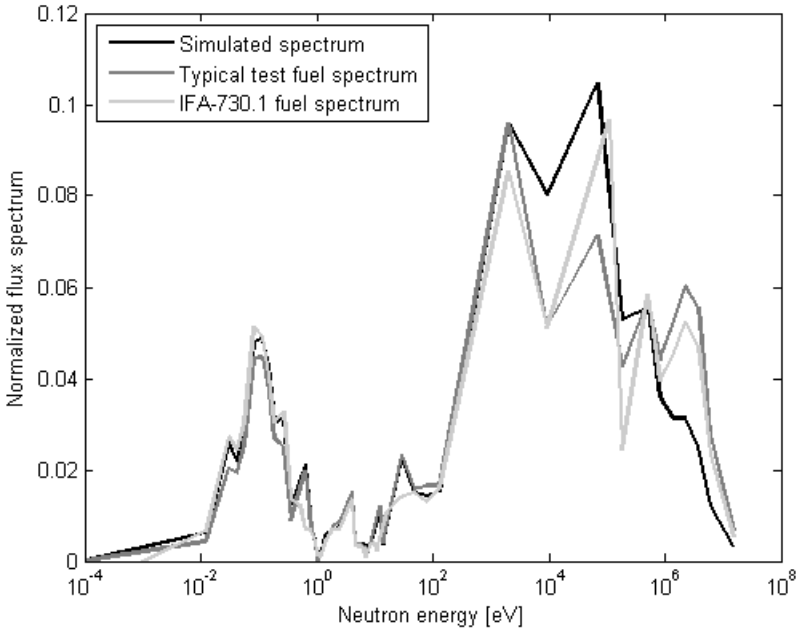

Figure 3.4: The flux in the HBWR and the simulated flux.

3.3.2 Reference cases

From the pin model in Serpent a set of reference cases was created. The reference cases varied a set of input parameters important for the shape of the power profile. These parameters, along with the range of their perturbation can be seen in Table 3.2. The exact compositions of plutonium are found in Table 3.3 .

61 reference cases were created for LWR conditions and 94 for HWR conditions. All these can be found in Appendix A. Not all possible cases could be created due to the large amount of possible cases and the time taken for each case to be finished. Serpent simulated the power profile for 17 different burnup steps. These were 0, 0.1, 0.5, 1, 2, 5, 10, 20, 25, 30, 35, 40, 45, 50, 60 and 70 $\frac{GWd}{tHM}$.

There were four different parameters to be evaluated and three to five different values for each, and the calculation time for each case was about seven to eight hours. To generate all possible cases would thus take several months, and therefore only a set of well representative cases were calculated and used in the evaluation.

Table 3.2: Parameters perturbed in the different cases together with the range of the change.

Parameter	Range
Outer radius	0.39 - 0.55 cm
Inner radius	0 - 0.12 cm
Plutonium fraction	5 - 18 %
Plutonium composition	50 - 90 % ^{239}Pu

Table 3.3: Concentration of isotopes for the different fuel compositions.

Name	^{238}Pu	^{239}Pu	^{240}Pu	^{241}Pu	^{242}Pu
Composition ”92”	0.012	91.551	8.309	0.085	0.044
Composition ”80” [6]	0.1	80	16.9	2.7	0.3
Composition ”59” [6]	2.6	59.8	23.7	10.6	3.3
Composition ”56” [6]	1.3	56.6	23.2	13.9	5
Composition ”50” [6]	2.7	50.4	24.1	15.2	7.5
Composition ”80n”	0	80	17	2	1
Composition ”65n”	0	65	20	10	5

3.4 Parameter determination

All the parameters needed to be determined are listed in Table 3.4 and Equation 3.1. C and D in Equation 3.1 are the parameters in the form function in Equation 2.16. The sheer amount of parameters made it very hard to use classical optimization algorithms, and therefore a GA was used, see Section 2.5. Encoding of the parameters was done using real numbers, creep mutation was employed and the initial population was chosen as a mutation of an initial guess. This was done due to the nature of the problem. As the parameters were roughly known from the previous model, an initial guess is superior to a random distribution. This was also an incentive to use real number encoding and creep mutation as these will change the values from the initial position instead of changing it more randomly as can be the case of a bit flip mutation. The initial guess and the creep rates are listed in Table 3, 4, 5, 6 in Appendix C.

The cross sections of the nuclides varied with a factor of about 100 and therefore the creep rate had to be adjusted so that small cross sections varied less than large cross sections, which gave a more stable convergence to the optimal value than using a constant creep rate.

The initial guess for LWR was obtained in two steps. First parameters from the model for Th-U proposed by Y.Long [16] were used to optimize the initial burnup for

one case. Secondly the set of parameters obtained from this was then used to optimize the same case with all burnup steps. This last set of parameters was used as the initial guess for the parameter determination. For HBWR the initial guess was chosen in the same manner.

Table 3.4: LWR cross sections in the GA.

Fission cross sections	Capture cross sections
$\sigma_{a,Th232}$	$\sigma_{c,Th233}$
$\sigma_{a,U233}$	$\sigma_{c,U233}$
$\sigma_{a,U234}$	$\sigma_{c,U234}$
$\sigma_{a,U235}$	$\sigma_{c,U235}$
$\sigma_{a,U236}$	$\sigma_{c,U236}$
$\sigma_{a,Pu238}$	$\sigma_{c,Pu238}$
$\sigma_{a,Pu239}$	$\sigma_{c,Pu239}$
$\sigma_{a,Pu240}$	$\sigma_{c,Pu240}$
$\sigma_{a,Pu241}$	$\sigma_{c,Pu241}$
$\sigma_{a,Pu242}$	$\sigma_{c,Pu242}$

$$\begin{aligned} C_1 &= Thp1 + Thp4 \cdot R \\ C_2 &= Thp2 \\ C_3 &= Thp3 \\ D_1 &= Pup1 + Pup7 \cdot R + Pup4 \cdot \tfrac{N_{Pu239} \cdot Z}{2.44 \cdot 10^{22}} \\ D_2 &= Pup2 + Pup5 \cdot \tfrac{N_{Pu239} \cdot Z}{2.44 \cdot 10^{22}} \\ D_3 &= Pup3 + Pup6 \cdot \tfrac{N_{Pu239} \cdot Z}{2.44 \cdot 10^{22}} \end{aligned} \tag{3.1}$$

For the LWR parameters 49 of the reference cases were used in the training set while 12 were used as the validation set. For the HBWR, 76 cases were used in the training set and 18 in the validation set. The GA uses several internal parameters for the optimization which are tabulated in Table 3.5

Table 3.5: The parameters for the GA.

Parameter	Value
Population size	100
Crossover probability	0.8
Tournament selection parameter	0.75
Mutation probability	1/31

4

RESULTS

4.1 Serpent simulation

The power profiles simulated with Serpent exhibit a resemblance to the profiles calculated by FRAPCON for normal UOX fuel, see Figure 4.1. It was not a perfect match though, especially not for high burnup where the deviation was up to 10 %. The fluctuations in the Serpent data are due to the stochastic nature of Monte Carlo simulations.

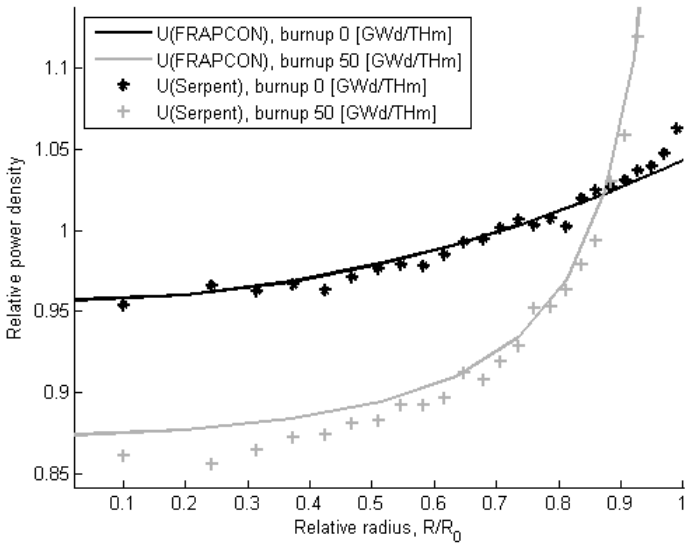

Figure 4.1: Comparison of power profile for uranium fuel for Serpent simulation and FRAPCON calculation with the TUBRNP model. The last radial points on the FRAPCON curve with a very high power density are cut out of this figure to display the details better.

Figure 4.2 shows the difference in behaviour of the Th-MOX and the UOX fuel. The standard uranium fuel has a flatter profile in the beginning but during irradiation the power increases drastically at the rim and decreases in the center. This is not observed in the Th-MOX fuel, which in the initial stage has a rather curved shape which during irradiation flattens out and only at very high burnup or with low Pu content increases at the rim.

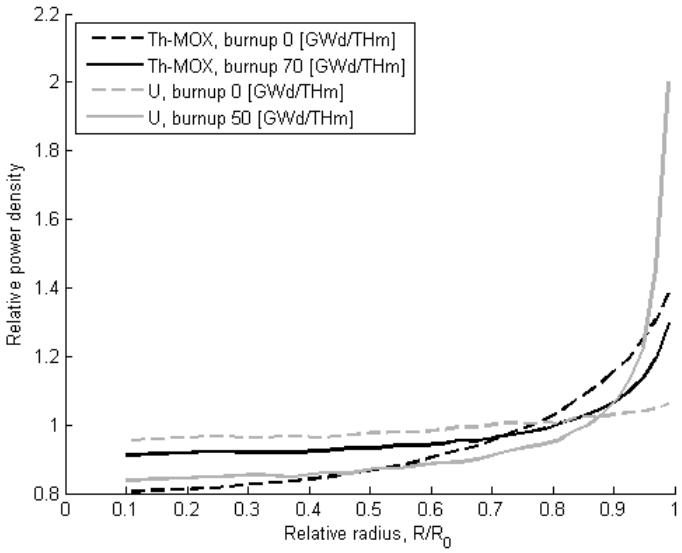

Figure 4.2: Comparison of power profile for uranium and thorium-plutonium fuel.

Figure 4.3 shows two different LWR cases with the same geometry but different fissile contents. The pin with the higher fissile content has a larger change in the shape of the power profile in the center of the pin, and the power at the rim does not change much. For the low fissile content pin, the change of the over all profile is smaller, but the power at the rim increases at medium to high burnup. The effect is more visible when the total content of Pu varies. The same difference can also be seen between two pins with different pin radius and pin pitch (to keep the H/HM ratio constant) but the same plutonium composition, as shown in Figure 4.4. The reference plutonium compositions can be found in Table 3.3

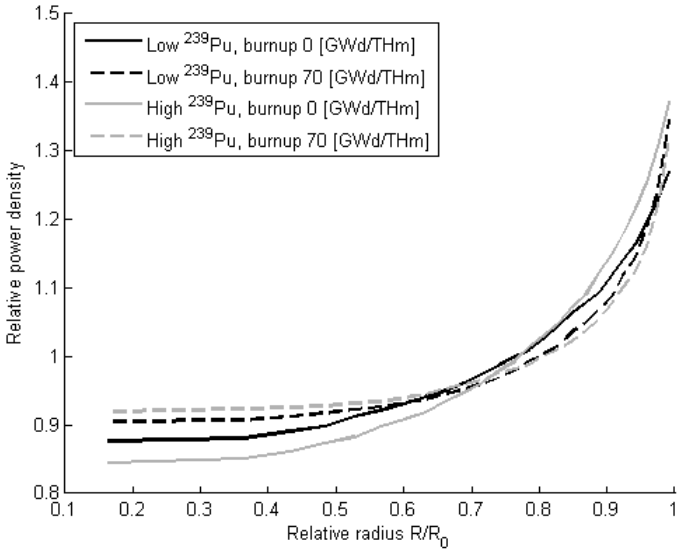

Figure 4.3: The power profile for two pins in LWR conditions. Both has a radius of 0.47 cm and a total Pu concentration of 8 %. The high Pu pin used composition ”92” while the low Pu used composition ”65n”.

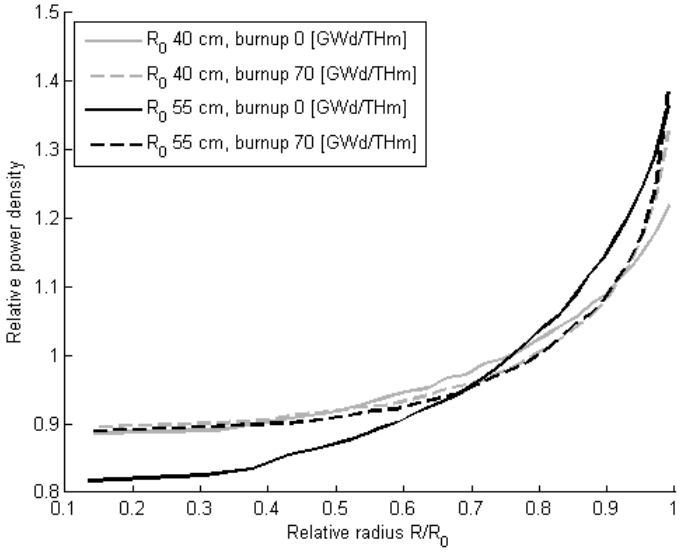

Figure 4.4: The power profile for two pins in LWR conditions. Both has a total plutonium content of 8 % and composition ”56”.

For pins in HBWR conditions the profiles are similar but with a larger difference between low and high burnup. In the cases with the largest amount of fissile Pu the

power was almost flat after 70 $\frac{GWd}{tHM}$, see Figure 4.5

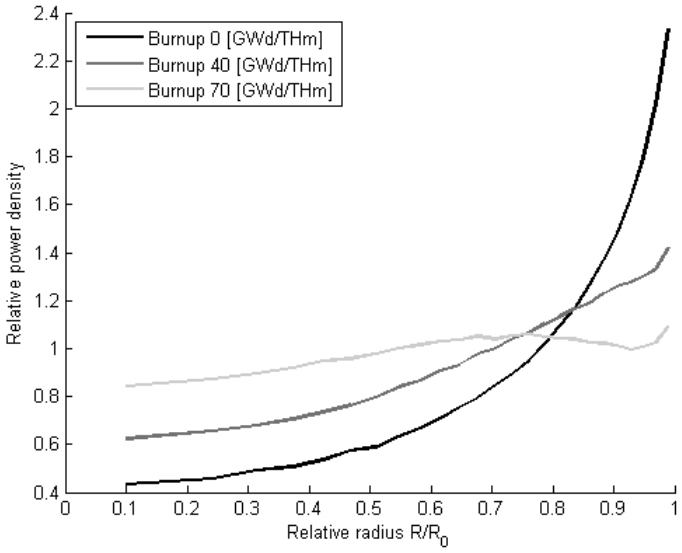

Figure 4.5: The radial power profile for HBWR conditions.

4.2 Parameter values

The final set of cross sections is shown in Table 4.1 and the coefficients for the final shape functions are shown in Equation 4.1 and 4.2. The approximate shapes of the shape functions can be found in Figure 4.6.

Figures 4.7 and 4.8 contain the validation and training fitness for the two GA calculations. The fitness for the training set increased a lot in the beginning and started to level out after a while as expected, see Figure 2.5. Fitness for the HBWR case had not got to steady state, which was due to time constraints. But it would not have increased very much more than it already had. The validation curves for both LWR and HBWR did not behave as expected. Instead of decreasing as predicted due to over fitting they behaved similar to the training set. This is discussed in Section 5.

Table 4.1: The final absorption and fission cross section for LWR and HBWR in the model.

Nuclide	σ_f LWR [barn]	σ_f HBWR [barn]	σ_c LWR [barn]	σ_c HBWR [barn]
^{232}Th	1.62	4.46	4.68	1.50
^{233}U	131	222	1.43	7.82
^{234}U	0.223	0.145	39.0	44.6
^{235}U	52.9	63.0	1.64	0.313
^{236}U	0.0368	0.4258	31.4	33.7
^{238}Pu	0.0568	0	148.4	292
^{239}Pu	44.7	108	30.7	53.7
^{240}Pu	0	0	0	357
^{241}Pu	125	31.5	211	283
^{242}Pu	0	0	98.3	216

$$C_1 = 0.7512 + 0.6260 \cdot R_0 \tag{4.1a}$$
$$C_2 = 2.4762 \tag{4.1b}$$
$$C_3 = 0.7166 \tag{4.1c}$$
$$D_1 = 0.7424 + 9.1746 \cdot R - 1.2564 \cdot \frac{N_{Pu239} \cdot Z}{2.44 \cdot 10^{22}} \tag{4.1d}$$
$$D_2 = 0.7555 + 5.2098 \cdot \frac{N_{Pu239} \cdot Z}{2.44 \cdot 10^{22}} \tag{4.1e}$$
$$D_3 = 0.7823 - 0.5485 \cdot \frac{N_{Pu239} \cdot Z}{2.44 \cdot 10^{22}} \tag{4.1f}$$

$$C_1 = 0.5889 + 2.5374 \cdot R_0 \tag{4.2a}$$
$$C_2 = 3.2832 \tag{4.2b}$$
$$C_3 = 0.8368 \tag{4.2c}$$
$$D_1 = 2.0229 + 24.2327 \cdot R - 13.2924 \cdot \frac{N_{Pu239} \cdot Z}{2.44 \cdot 10^{22}} \tag{4.2d}$$
$$D_2 = 0.3211 + 6.6294 \cdot \frac{N_{Pu239} \cdot Z}{2.44 \cdot 10^{22}} \tag{4.2e}$$
$$D_3 = 0.5205 + 2.3236 \cdot \frac{N_{Pu239} \cdot Z}{2.44 \cdot 10^{22}} \tag{4.2f}$$

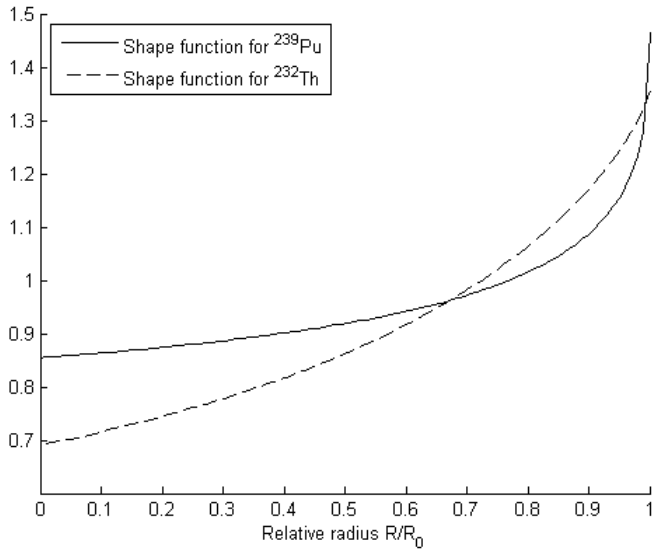

Figure 4.6: The approximate shapes of the shape functions.

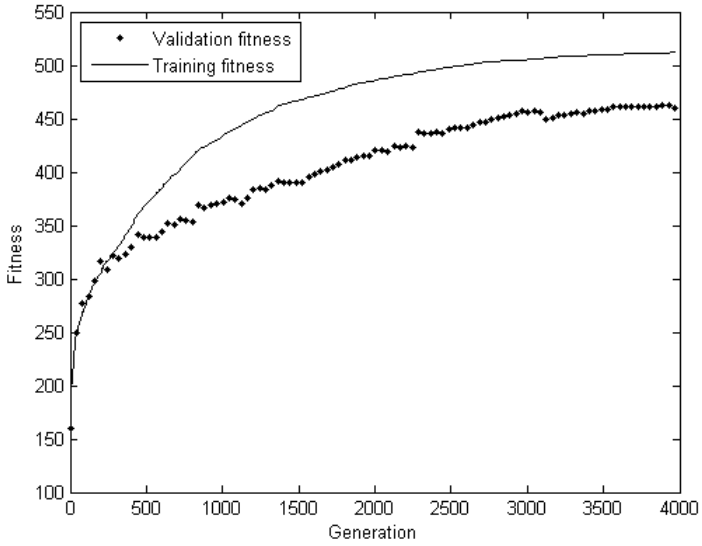

Figure 4.7: Fitness of the validation and training set during the GA calculation for LWR.

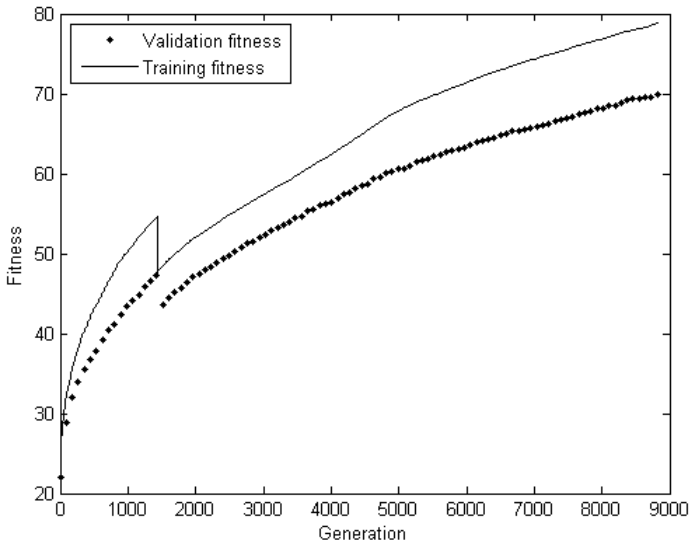

Figure 4.8: Fitness of the validation and training set during the GA calculation for HBWR. The discontinuity at generation 1500 comes from an addition of new reference cases.

4.3 The new model

Figures 4.9 - 4.10 show some configurations of fuel pins in LWR conditions and how well the new subroutine performed with the new set of parameters. As can be seen, for pins with a large radius it overestimated the power in the centre for low burnup and underestimated it for high burnup. The opposite was observed for pins with a small radius. This was true for many, but far from all cases, as the Pu composition also played a large role.

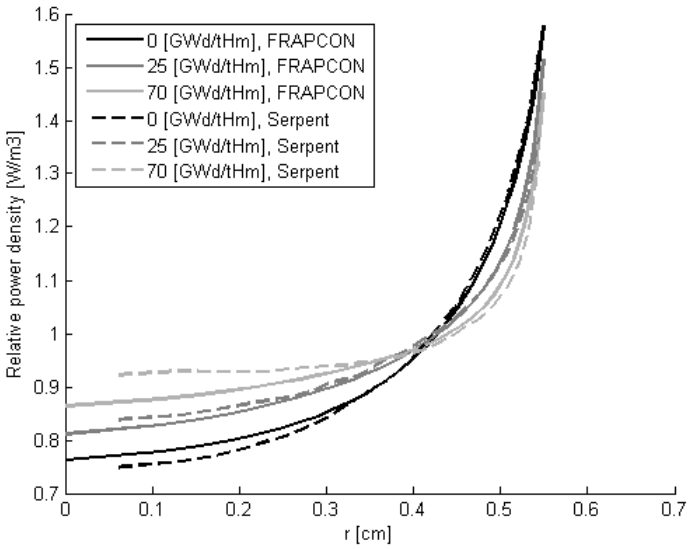

Figure 4.9: The radial power profile for a pin with radius 0.55 cm, pitch of 1.688 cm, a plutonium content of 8 % and the plutonium composition "92" for a LWR case.

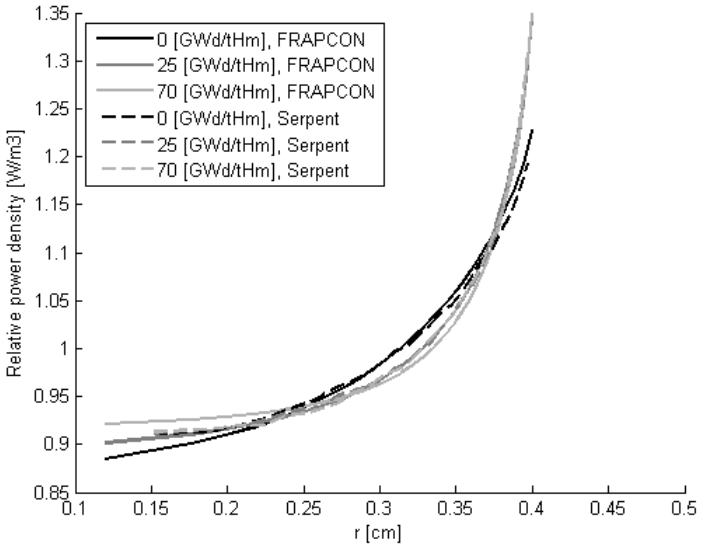

Figure 4.10: The radial power profile for a pin with radius 0.40 cm, pitch of 1.16 cm, plutonium content of 8 % and plutonium composition "65n" for a LWR case.

For HBWR conditions the overall result was worse than for LWR conditions. Pins with a high amount of ^{239}Pu, as in composition "92" performed worse that the pins with the other compositions, see Figures 4.11 and 4.12. This will be discussed in Section 5.

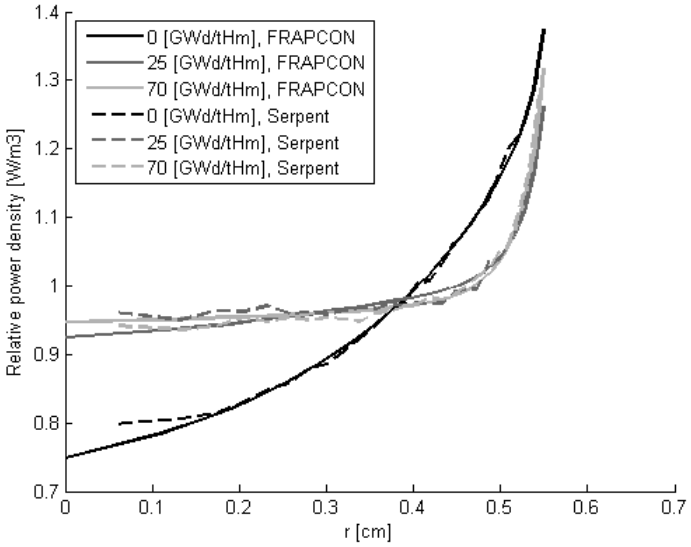

Figure 4.11: The power profile of a pin with radius 0.55 cm, plutonium content of 8 % and plutonium composition "56" for a HBWR case.

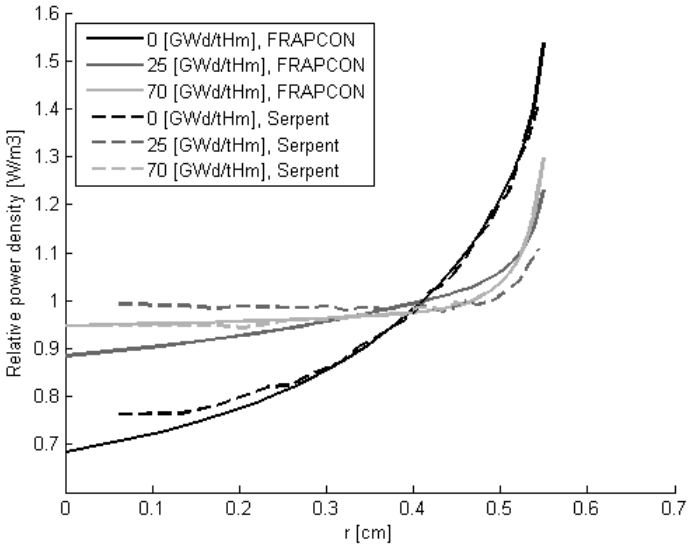

Figure 4.12: The power profile of a pin with radius 0.55 cm, plutonium content of 8 % and plutonium composition "92" for a HBWR case.

4.3.1 Statistics

Figures 4.13 and 4.14 show the relative error in % for all radial nodes, burnup steps and all cases. The error was calculated using Equation 4.3. For LWR the mean relative error, μ was 0.57 % and the standard deviation, σ, was 0.57 %. Over 99.9 % of all nodes fell within an error of 5 % and over 84 % fell within 1 % error. The values for HBWR was μ = 1.58 %, σ = 1.51 %, 96 % and 45 % fell within 5 and 1 % error respectively. Figure 4.15 shows the absolute error for LWR and figure B.4 for a HBWR. The shape of the curve is symmetric, indicating that the error was not skewed towards negative or positive values.

$$e = \frac{|P_{FRAPCON} - P_{Serpent}|}{P_{Serpent}} \tag{4.3}$$

Figures 4.16 and 4.17 show the relative error and the standard deviation for the different radial positions in the fuel pins. The absolute error as well as the standard deviation was lowest between the middle and the rim of the pin. The relative error was larger at the rim than at the centre. Both curves have the same shape and follow each other closely. This is true for both HBWR and LWR.

Figures 4.18 and 4.19 show the relative error and standard deviation for different burnup steps for all fuel pins. The model performs best in LWR conditions at low burnup. For HBWR the performance is best at really low burnup and at really high burnup.

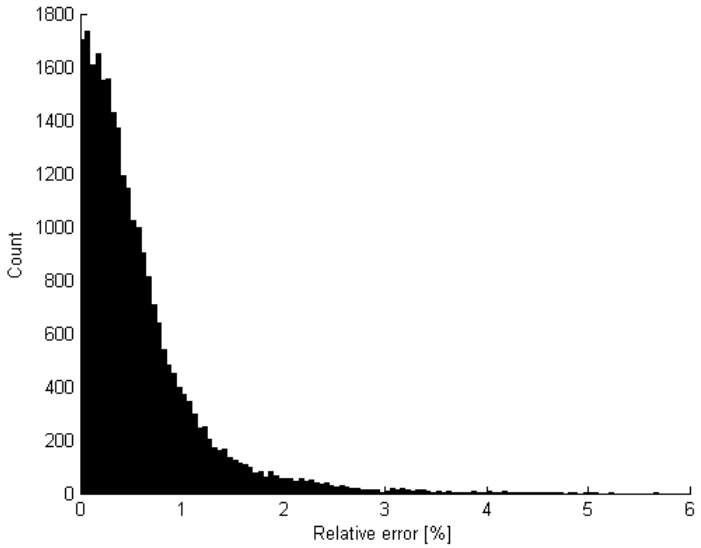

Figure 4.13: The relative error for all nodes of all pins for LWR.

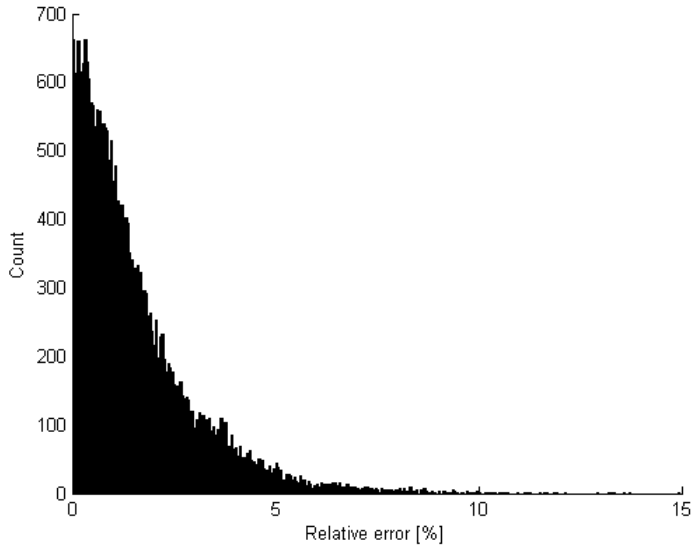

Figure 4.14: The relative error for all nodes of all pins for HBWR.

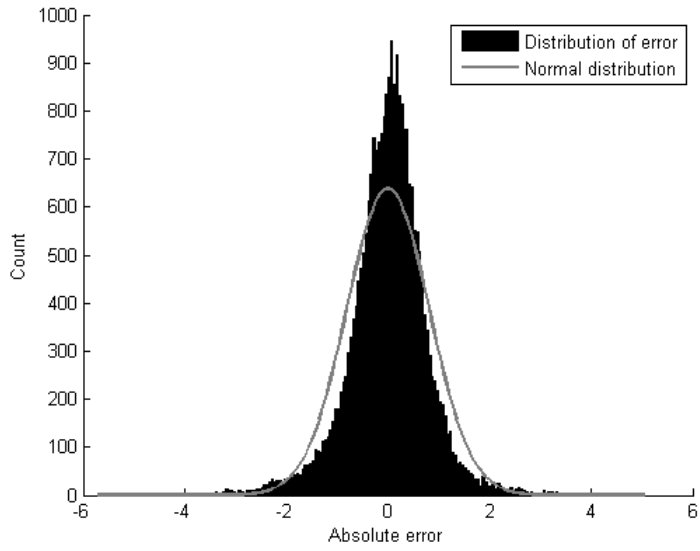

Figure 4.15: The absolute error for all nodes of all pins for LWR.

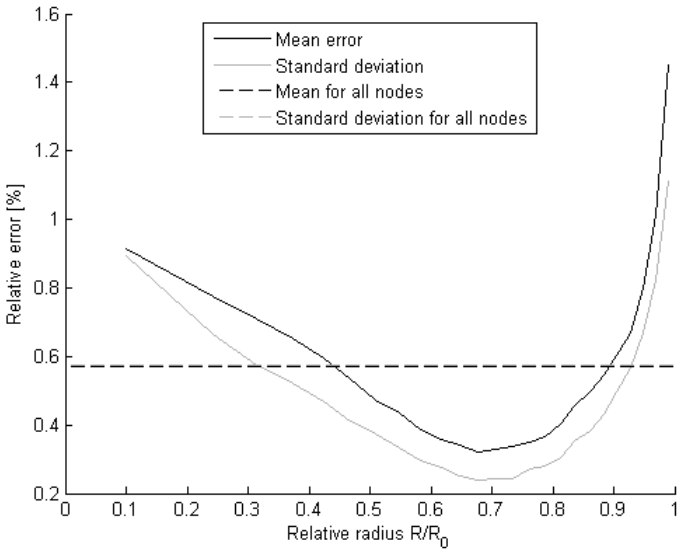

Figure 4.16: The relative error for different radial positions in LWR cases. The relative radius neglects the hole in the hollow pins.

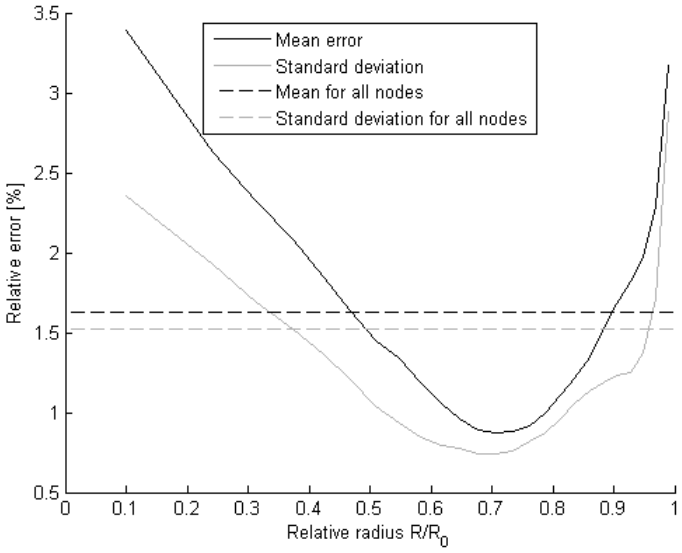

Figure 4.17: The relative error for different radial positions in HBWR cases. The relative radius neglects the hole in the hollow pins.

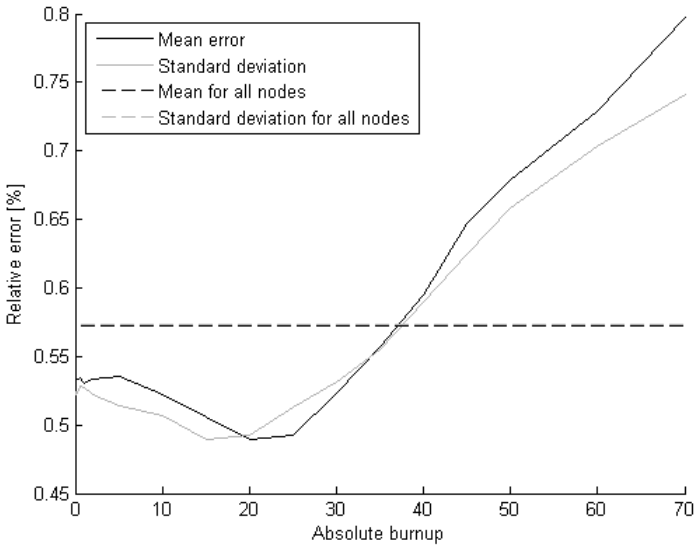

Figure 4.18: The relative error for all burnup steps for LWR.

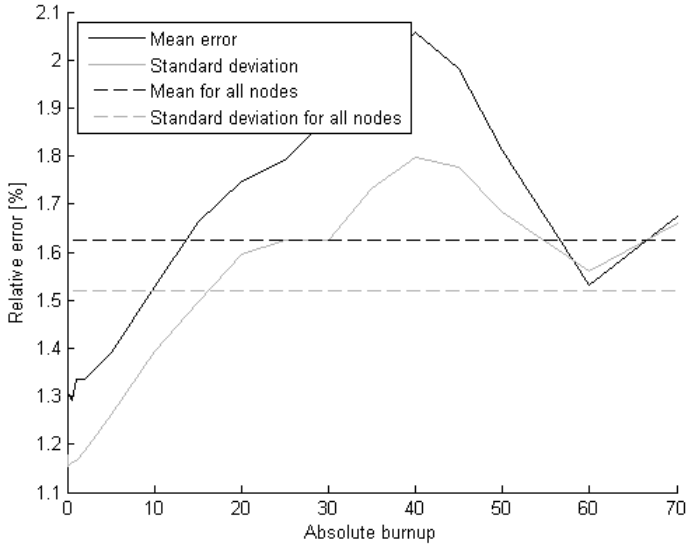

Figure 4.19: The relative error for all burnup steps for HBWR.

4.3.2 Comparison with experimental data

Figure 4.20 shows the difference in centre temperature of a hollow Th-MOX fuel pin calculated with both TUBRNP and TTPBRN. The parameters of the fuel pin are listed in Table 4.2. There was a small difference of only a few tens of °C, but the new subroutine

performed better than the old one by decreasing the over-prediction at temperatures representative of commercial LWR operation, i.e. the higher measured temperature. The fuel material densification during the initial stages of the irradiation is not considered yet in the FRAPCON version used for these calculations, so the result may change slightly as that is dealt with. The deviation of the calculated temperature from the measured data after 50 days is due to the fact that the burnup dependence of the material property correlations is not yet adapted to Th-MOX fuel behaviour.

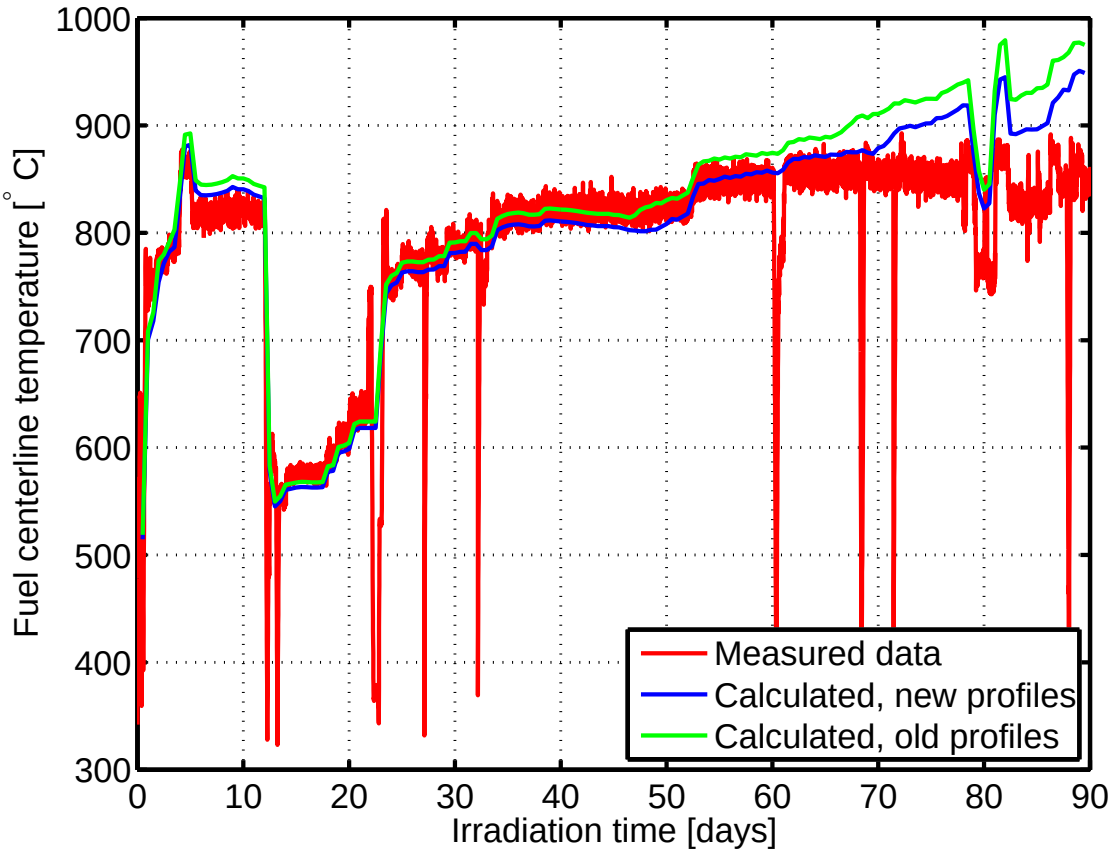

Figure 4.20: The centerline temperature calculated with the new and old model, compared to the measured value from the Halden research reactor.

Table 4.2: Parameters of the irradiated pin.

Parameter	Value
Outer radius	0.294 cm
Inner radius	0.12 cm
Plutonium fraction	7.92 %

5

DISCUSSION

5.1 Serpent simulation

The data collected is assumed to be reasonably correct since Monte Carlo simulations in general have a good accuracy, provided good cross section libraries. Serpent has been validated by comparison to MCNP running some standard assembly calculation problems [4]. To fully validate the reference data one would need test irradiation of thorium rods and compare the isotopic compositions for the different radial positions.

The number of reference cases was chosen both to meet the requirements for the amount of data for the GA and the time needed to gather and analyze it. The time requirement could have been circumvented to some extent by making a more thorough investigation of the precision needed in the simulation and more efficient use of the Matlab code. After the parameter determination some new cases were added to the reference set. These cases were solved well with the old set of parameters, indicating that the amount of reference cases was large enough.

The dimensions in the reference cases were constrained to a radius between 0.39 and 0.55 mm. This was because this is the normal range in which fuel pins are fabricated [23]. The range of the concentration of plutonium was chosen as the range most likely to be used and the composition was chosen as the normal composition from various reactors and from nuclear weapons. Other concentrations and compositions were considered unnecessary for the parameter adaptation.

These constraints were made to decrease the amount of reference cases and to make the model more adapted to real cases, as well as reducing the time consumed for data generation. There are no underlying assumptions or limitations in the model that prevents usage of the code outside the range of the reference data in Table 3.2, and exceeding these will probably work, but the test cases used to generate data for the model have not been varied outside. Thus exceeding the limitations will be risky. Increasing the Pu concentration beyond 20 % will not work very well, but decreasing it and changing the

radius works quite well, see Figure 5.1 and 5.2.

Dimensions for the cladding and cladding gap were also not a part of the radial power profile model, but had to be included in the model in Serpent. The effect of this was not large and could safely be neglected in the new model, see Figure B.3.

For the LWR case no difference was made between BWR and PWR. The conditions, especially the H/HM ratio, were considered similar enough to lump together into one model. Typical values of the H/HM ratio are around 2.6 for PWR and 2.2 for BWR and a value of around 2.2 was used. This assumption is also used by Y.Long [16] and in the OMICO project [13].

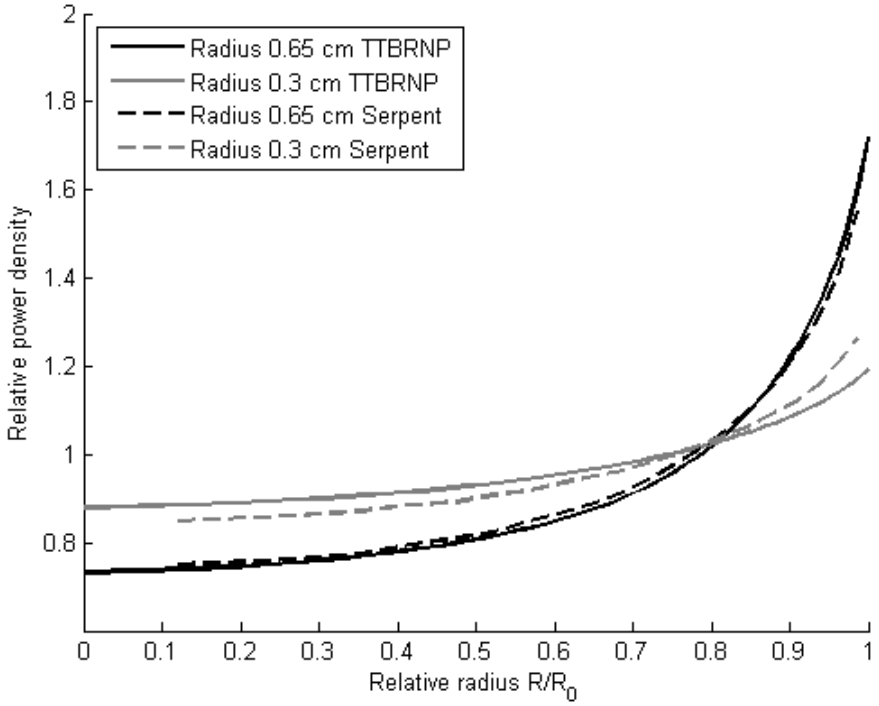

Figure 5.1: Calculated and simulated cases outside of the limitation of the model. Plutonium concentration is here 8 % and with composition "92".

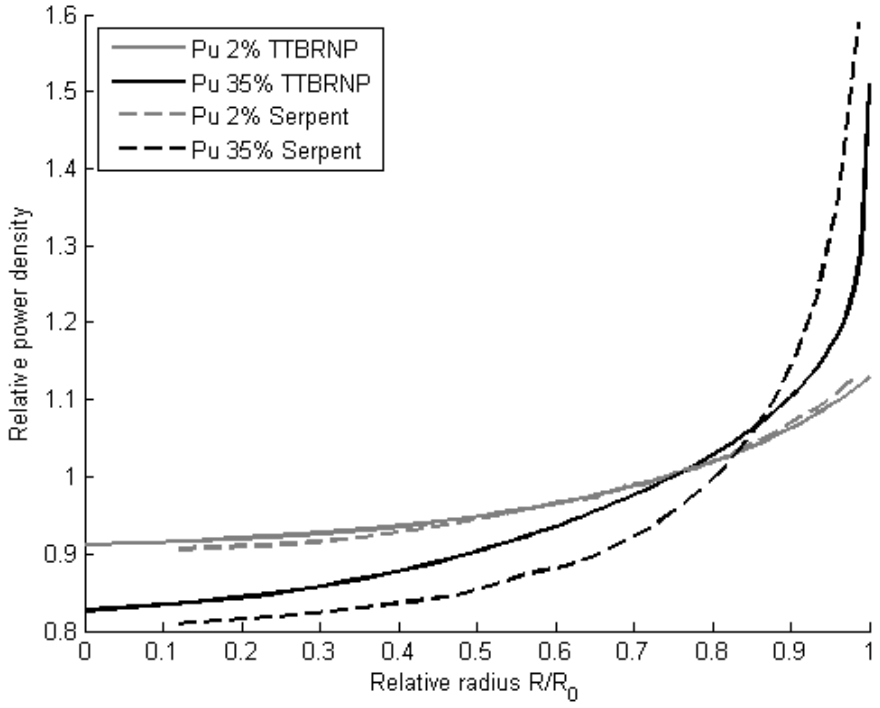

Figure 5.2: Calculated and simulated cases outside of the limitation of the model. Radius is here .43 cm and with composition "92".

5.2 Parameter values (GA)

Some of the parameters adapted by the GA were very different compared to previous models for Th-U fuel [16]. One case is the low fission cross sections for plutonium and the high fission cross section for ^{233}U, but also many of the capture cross sections were somewhat different, see Table 5.1. The most problematic difference is the capture cross section of ^{240}Pu, for which the genetic algorithm found a value of 0. This is highly unreasonable, especially as the real thermal capture cross section is in the same order as for the other Pu isotopes. The problem may be that the model does not describe the plutonium burnup very well. It may also be that the genetic algorithm finds values for the shape functions that compensates for the cross section and thereby gets stuck in a local optimum. One could possibly get around this problem by adapting the shape function separately, using measured atomic densities in real irradiated pins of different burnups.

There are many other circumstances contributing to these differences. One thing is the way the shape function is implemented. This changes the conditions in the model and therefore the average cross sections must inevitably change. Some more nuclides are also present which change the absorption of the neutrons. A particular resonance

peak in one isotope might alter the total absorption in another in a way that is hard to predict. There are also some empirical correlations in the new model not present in the others, which change the requirements for the cross sections. Most notable though may be the way the cross sections were calculated. The genetic algorithm finds a solution to the problem, in this case adapting cross sections to fit a curve, without regards of any physical phenomena.

The atomic densities are only used inside the subroutine itself. Because of this they were not used for the purpose of cross section and shape function parameter determination. If these also were used as feedback to the genetic algorithm a more realistic set of parameters probably would be obtained, not necessarily better though.

Table 5.1: The cross sections for the model proposed by Y.Long [16] and for LWR in the TTPBRN subroutine.

Nuclide	σ_f TTPBRN	σ_f Y.Long model	σ_a TTPBRN	σ_a Y.Long model
^{232}Th	1.62	0	4.68	1.6
^{233}U	131	64	1.43	8
^{234}U	0.223	1	39.0	27
^{235}U	52.9	41.5	1.64	10.3
^{236}U	0.037	0.73	31.4	17.7
^{239}Pu	44.7	115	30.6562	63
^{240}Pu	0.	0.584	0	100.
^{241}Pu	125	120	211	50.
^{242}Pu	0.	0.458	98.3	80.

The fitness values for the validation set did not behave as expected. Instead of increasing in the beginning and declining after a while it increased steadily all the time. There can be some reasons for this. Either the GA did not run for a long enough time so that the fitness for the validation set had time to decline, which is most probably not the case for LWR, and likely not the case for HBWR. Even though it did not run for enough generations, there is no reason to suspect it would turn out differently. Or the different reference cases were so similar that there really was just one set of parameters describing them all in the best way, and by finding the best set for the majority of the reference cases the best set for the validation cases was found at the same time.

The reason why the GA did not run any longer for the LWR cases was that the improvement of the parameter set was very slow and was going to a halt. Very little improvement over what had already happened was expected, see Figure 4.7. For HBWR the reason was mainly time limitation, and that the performance was not expected to increase very much.

5.3 The TTPBRN model

The reason the shape function was changed and implemented for Pu and Th was to take care of the problem that the initial model could not predict the power profile during low burnup. The old model performed well for high burnup, but this was probably due to overcompensation from the shape function and Pu/U production. This was partly due to the added thorium but mostly because of the plutonium. Both plutonium and thorium have larger absorption cross sections than uranium, which might render Fick's law, and thereby the diffusion approximation invalid, [13]. The resonance peaks in ^{239}Pu probably also play a role in the differences as they increased the epithermal absorption. It is surprising why this has not been considered before, as the old FRAPCON model could be used to simulate plutonium containing fuel. Maybe the difference was not considered large enough to be important, or the problem was not noticed.

The numerical solution made it possible to calculate the neutron flux in a pin with radially varying atomic density. It did on the other hand introduce a numerical and systematic error. The question is whether these errors were smaller than the error of the previous model. The model became much better with the numerical method, and the systematic errors, which are an effect of the Cartesian coordinates used during calculation, is compensated for with the normalization and are small. The numerical errors are also small if enough radial nodes are used.

A majority of the reference cases for LWR were reproduced very well with the new model. Over 99.9 % of the data points fell within 5 % of the Serpent value. The model underperformed only in a few cases. It is hard to see a correlation between these underperforming cases. Many of them had a large radius, but on the other hand, most cases with a large radius did not underperform, indicating that it was the combination of certain plutonium concentrations together with certain radii which the model could not handle well. This could probably also be addressed, like the problem with the fuel to moderator ratio, with a more advanced model, for example more neutron energy groups and the modelling of the moderator as well. The problem with this is the same as before as it would be harder to find all cross sections and it could take too long time to perform the calculation for the purpose of which it is intended. There is also a possibility of putting more empirical correlations into the model, but this would probably make the model less general.

For HBWR the model did not perform as well as for LWR. Especially for pins with high ^{239}Pu concentration. This indicates that the model could be developed further and that the empirical methods may not be very good.

The model did not perform the same for all positions in the fuel, but better for the relative radius of about 0.7 and worse at the rim and middle. This indicates further that the model can be improved, especially concerning the empirical shape functions. How this could be made without increasing the computational burden too much or introducing even more empirical correlations is hard to tell.

5.4 Comparison with experimental data

The new subroutine gave a lower calculated value of the centre temperature of a Th-MOX fuel pin, shown in Figure 4.20. This was expected since the relative power was lower in the centre with the new subroutine compared to the old, see Figure 4.2.

It is difficult to assess whether or not the new subroutine does give a good approximation since the power profile only plays a small role in the centre line temperature prediction, but as mentioned before the solution agrees better with measured data at typical temperatures so this is probably the case.

5.5 Further work

There is some work left to be done. The code needs to be validated using experimental post irradiation data. The radial distribution of the isotopes in an irradiated pin would be useful. Also the genetic algorithm could be improved further by incorporating the atomic densities as feedback. The model would probably perform a little bit worse, but the cross sections would be more accurate.

6

CONCLUSIONS

The new model, TTPBRN predicted the radial power profile very well for LWRs, with little deviation from the results simulated by Serpent. A relative error of 0.57 % was observed. The results for HBWR was not equally good, with a relative error of 1.58 %. Least errors compared to Serpent simulations were found at a relative radius of 0.7. It did not perform equally well in all positions in the pin, which indicates that the calculation method is not perfect.

The GA could be improved by utilizing the atomic densities in the parameter determination to get a more realistic value for the cross sections, as some of these were unphysical.

Integration of the TTPBRN into FRAPCON gives a lower and seemingly better prediction of the centreline temperature, but more work needs to be done on other parts of the FRAPCON code to be certain of its actual effect. [14]

Bibliography

[1] World Nuclear Association, Mixed oxide (MOX) fuel (May 2014).
URL http://www.world-nuclear.org/info/Nuclear-Fuel-Cycle/Fuel-Recycling/Mixed-Oxide-Fuel-MOX/

[2] Thor Energy, Thorium as nuclear fuel (May 2014).
URL http://www.thorenergy.no/no/Topmenu/Thorium/Challenges-and-possibilities.aspx

[3] K.Geelhood, W. Luscher, C.Beyer, FRAPCON-3.4: A Computer Code for the Calculation of Steady-State Thermal-Mechanical Behavior of Oxide Fuel Rods for High Burnup, United States Nuclear Regulatory Commission, Pacific Northwest National Laboratory, P.O. Box 999, Richland, WA 99352 (March 2011).

[4] J. Leppänen, Serpent – a Continuous-energy Monte Carlo Reactor Physics Burnup Calculation Code, VTT Technical Research Centre of Finland (August 2012).

[5] V. McLane, et al., Endf-I02 dataformats and procedures for the evaluated nuclear data file endf-6, Tech. rep., National Nuclear Data Center.

[6] World Nuclear Association, Mixed oxide (mox) fuel (May 2014).
URL http://www.world-nuclear.org/info/Nuclear-Fuel-Cycle/Fuel-Recycling/Plutonium/

[7] World Nuclear Association, Mixed oxide (mox) fuel (May 2014).
URL http://www.world-nuclear.org/info/Nuclear-Fuel-Cycle/Uranium-Resources/Military-Warheads-as-a-Source-of-Nuclear-Fuel/

[8] J. Magill, G.Pfennig, J.Galy, Karlsruher nuklidkarte, 7th edition, Tech. rep., European Commission, Joint Research Centre (2006).

[9] World Nuclear Association, Mixed oxide (mox) fuel (May 2014).
URL http://www.world-nuclear.org/info/Current-and-Future-Generation/Thorium/

[10] NNDC, Evaluated nuclear data file (endf) retrieval and plotting (December 2011).
URL `http://www.nndc.bnl.gov/sigma/index.jsp?as=1&lib=endfb7.0&nsub=10`

[11] J. R. Lamarsh, Introduction to Nuclear Reactor Theory, American Nuclear Society, Inc., 2002.

[12] V. Arkhipov, Thorium based fuel options for the generation of electricity: Developments in the 1990s, Tech. rep., IAEA (2000).

[13] S. Lemehov, K. Govers, Radial power distributions in (Th,Pu)O2 fuel pins and comparison with UO2 and MOX, Tech. rep. (March 2007).

[14] K. Lassmann, C. O'Carroll, CT. Walker, J. van de Laar, The radial distribution of plutonium in high burnup uo, fuels., Journal of Nuclear Materials.

[15] C. Demazière, Physics of Nuclear Reactors, Division of Nuclear Engineering, Department of Applied Physics, Chalmers University of Technology, Gothenburg, Sweden., 2012.

[16] Y. Long, Modeling the performance of high burnup thoria and urania pwr fuel, Ph.D. thesis, Massachusetts Institute of Technology (June 2002).

[17] National Science Foundation, LAPACK, Linear Algebra PACKage (November 2013).
URL `http://www.netlib.org/lapack/`

[18] M. Wahde, Biologically Inspired optimization Methods., WIT Press, Ashurst Lodge, Ashurst, Southampton, SO40 7AA, UK, 2008.

[19] K. Jareteg, Monte carlo simulations - lectures, Lecture notes (2013).

[20] E.W. Weisstein, Weak law of large numbers, from MathWorld–A Wolfram Web Resource (May 2014).
URL `http://mathworld.wolfram.com/WeakLawofLargeNumbers.html`

[21] E.W. Weisstein, Central limit theorem, from MathWorld–A Wolfram Web Resource (May 2014).
URL `http://mathworld.wolfram.com/CentralLimitTheorem.html`

[22] I. Lux, L. Koblinger, Particle Transport Methods: Neutron Photon Calculations, CLC Press, Inc., 2000 Corporate Blvd. N.W., Boca Raton, Florida 33431, 1991.

[23] J. Rhodes, K. Smith, D. Lee, CASMO-5/CASMO-5M, a Fuel Assembly Burnup Program, User's Manual, Studsvik Scandpower, sSP-07/431 (2007).

[24] S.Nøvik, Halden research project, personal communication (April 2014).

APPENDIX

A Reference cases

Table 1: Reference cases used for parameter determination for LWR.

R [cm]	R_0 [cm]	Pin pitch	Pu fraction [mass %]	Pu composition
0.43	0	1.295	0.0792	”92”
0.55	0	1.688	0.0792	”92”
0.55	0.12	1.63	0.0792	”92”
0.43	0	1.295	0.05	”92”
0.43	0	1.295	0.1	”92”
0.43	0	1.295	0.08	”65n”
0.55	0	1.688	0.08	”65n”
0.43	0	1.295	0.2	”92”
0.55	0	1.688	0.2	”92”
0.43	0	1.295	0.13	”92”
0.43	0	1.295	0.17	”92”
0.43	0	1.295	0.08	”80n”
0.5	0	1.52	0.08	”80n”
0.55	0	1.688	0.08	”80n”
0.4	0.12	1.16	0.08	”65n”
0.47	0.12	1.381	0.08	”65n”
0.55	0.12	1.632	0.08	”65n”
0.4	0.12	1.16	0.08	”92”
0.47	0.12	1.381	0.08	”92”
0.55	0.12	1.632	0.08	”92”
0.55	0	1.688	0.1	”59”
0.55	0	1.688	0.1	”59”
0.55	0	1.688	0.1	”50”
0.55	0	1.688	0.1	”80”
0.4	0	1.228	0.1	”59”
0.4	0	1.228	0.1	”59”
0.4	0	1.228	0.1	”50”

R [cm]	R_0 [cm]	Pin pitch	Pu fraction [mass %]	Pu composition
0.4	0	1.228	0.1	”80”
0.47	0	1.45	0.1	”92”
0.47	0	1.45	0.1	”59”
0.47	0	1.45	0.1	”59”
0.47	0	1.45	0.1	”50”
0.47	0	1.45	0.1	”80”
0.4	0	1.234	0.18	”50”
0.47	0	1.45	0.18	”50”
0.55	0	1.688	0.18	”50”
0.4	0	1.234	0.18	”80”
0.47	0	1.45	0.18	”80”
0.55	0	1.688	0.18	”80”
0.4	0	1.234	0.13	”50”
0.47	0	1.45	0.13	”50”
0.55	0	1.688	0.13	”50”
0.4	0	1.234	0.13	”80”
0.47	0	1.45	0.13	”80”
0.55	0	1.688	0.13	”80”
0.4	0	1.234	0.05	”59”
0.47	0	1.45	0.05	”59”
0.55	0	1.688	0.05	”59”
0.4	0	1.234	0.05	”50”
0.47	0	1.45	0.05	”50”
0.55	0	1.688	0.05	”50”
0.4	0.12	1.16	0.08	”50”
0.55	0.12	1.632	0.08	”50”
0.4	0.06	1.215	0.08	”50”

R [cm]	R_0 [cm]	Pin pitch	Pu fraction [mass %]	Pu composition
0.55	0.06	1.679	0.08	”50”
0.4	0.06	1.184	0.05	”59”
0.47	0.06	1.432	0.05	”59”
0.55	0.06	1.679	0.05	”59”
0.4	0.06	1.184	0.17	”59”
0.47	0.06	1.432	0.17	”59”
0.55	0.06	1.679	0.17	”59”

Table 2: Reference cases used for parameter determination for HBWR.

R [cm]	R_0 [cm]	Pu fraction [mass %]	Pu composition
0.43	0	8	”92”
0.39	0	5	”92”
0.39	0	5	”80”
0.39	0	5	”56”
0.47	0	5	”92”
0.47	0	5	”80”
0.47	0	5	”50”
0.55	0	5	”92”
0.55	0	5	”56”
0.55	0	5	”50”
0.39	0	8	”92”
0.39	0	8	”80”
0.39	0	8	”50”
0.47	0	8	”92”
0.47	0	8	”56”
0.47	0	8	”50”
0.55	0	8	”80”
0.55	0	8	”56”
0.55	0	8	”50”
0.39	0	10	”92”
0.39	0	10	”56”
0.39	0	10	”50”
0.47	0	10	”80”
0.47	0	10	”56”
0.47	0	10	”50”
0.55	0	10	”80”
0.55	0	10	”59”
0.55	0	10	”50”
0.39	0	14	”80”
0.39	0	14	”59”
0.39	0	14	”56”
0.47	0	14	”80”

R [cm]	R_0 [cm]	Pu fraction [mass %]	Pu composition
0.47	0	14	”59”
0.47	0	14	”50”
0.55	0	14	”80”
0.55	0	14	”56”
0.55	0	14	”50”
0.39	0	18	”80”
0.39	0	18	”59”
0.39	0	18	”56”
0.47	0	18	”80”
0.47	0	18	”59”
0.47	0	18	”50”
0.55	0	18	”80”
0.55	0	18	”56”
0.55	0	18	”50”
0.47	0.06	5	”92”
0.47	0.06	5	”80”
0.47	0.06	5	”50”
0.47	0.12	5	”92”
0.47	0.12	5	”80”
0.47	0.12	5	”50”
0.55	0.06	5	”92”
0.55	0.06	5	”56”
0.55	0.06	5	”50”
0.55	0.12	5	”92”
0.55	0.12	5	”56”
0.55	0.12	5	”50”
0.55	0.06	8	”80”
0.55	0.06	8	”56”
0.55	0.06	8	”50”
0.55	0.12	8	”80”
0.55	0.12	8	”56”
0.55	0.12	8	”50”

R [cm]	R_0 [cm]	Pu fraction [mass %]	Pu composition
0.47	0.06	10	”80”
0.47	0.06	10	”56”
0.47	0.06	10	”50”
0.47	0.12	10	”80”
0.47	0.12	10	”56”
0.47	0.12	10	”50”
0.55	0.06	10	”80”
0.55	0.06	10	”59”
0.55	0.06	10	”50”
0.55	0.12	10	”80”
0.55	0.12	10	”59”
0.55	0.12	10	”50”
0.55	0.06	14	”80”
0.55	0.06	14	”56”
0.55	0.06	14	”50”
0.55	0.12	14	”80”
0.55	0.12	14	”56”
0.55	0.12	14	”50”
0.47	0.06	18	”80”
0.47	0.06	18	”59”
0.47	0.06	18	”50”
0.47	0.12	18	”80”
0.47	0.12	18	”59”
0.47	0.12	18	”50”
0.55	0.06	18	”80”
0.55	0.06	18	”56”
0.55	0.06	18	”50”
0.55	0.12	18	”80”
0.55	0.12	18	”56”
0.55	0.12	18	”50”

B Sensitivity analysis cases

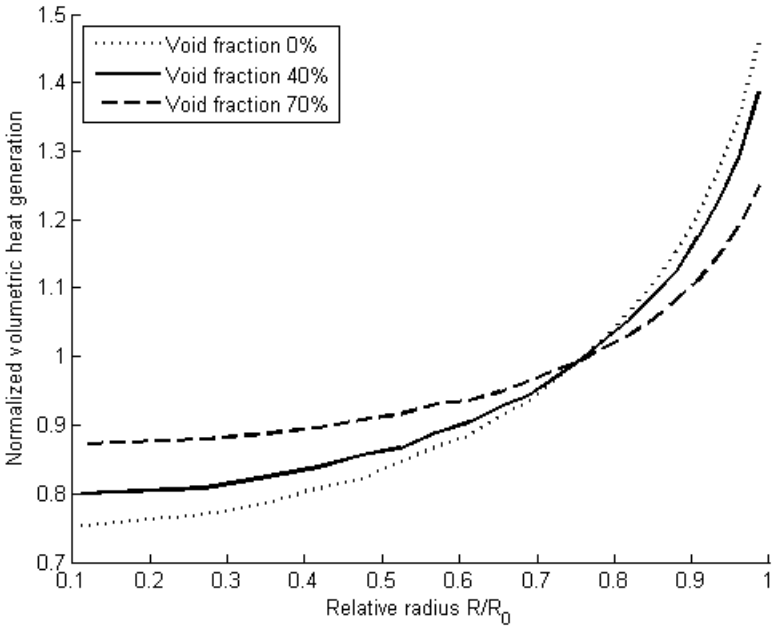

Figure B.1: The sensitivity for the moderator void fraction.

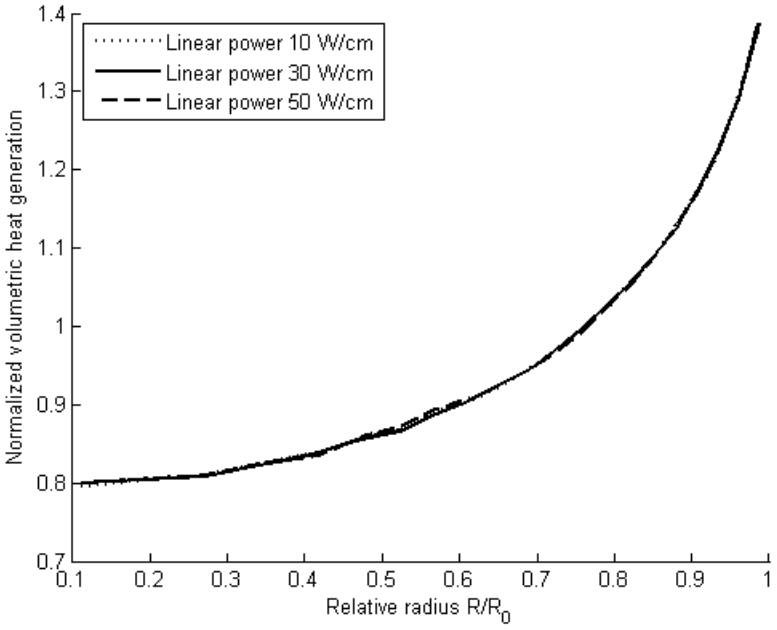

Figure B.2: The sensitivity for the linear hear generation rate in the fuel pin.

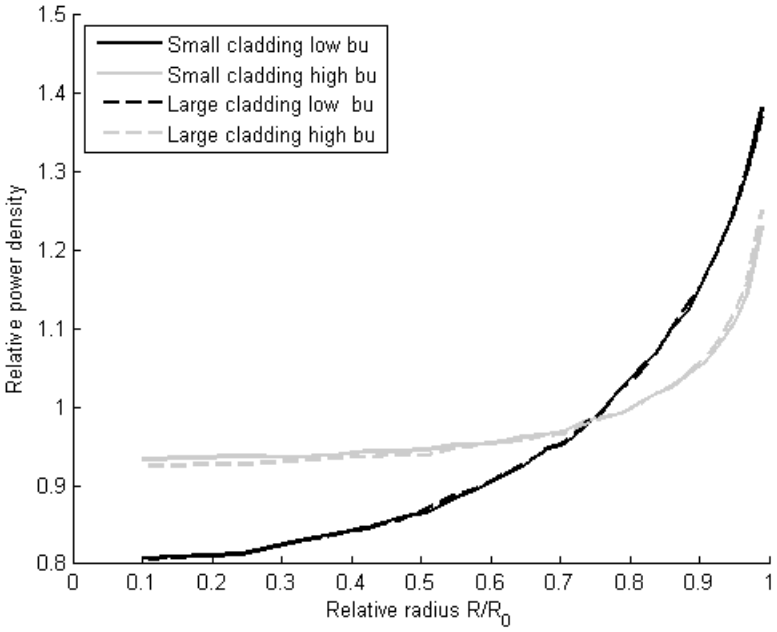

Figure B.3: The sensitivity for the cladding thickness of the fuel pin.

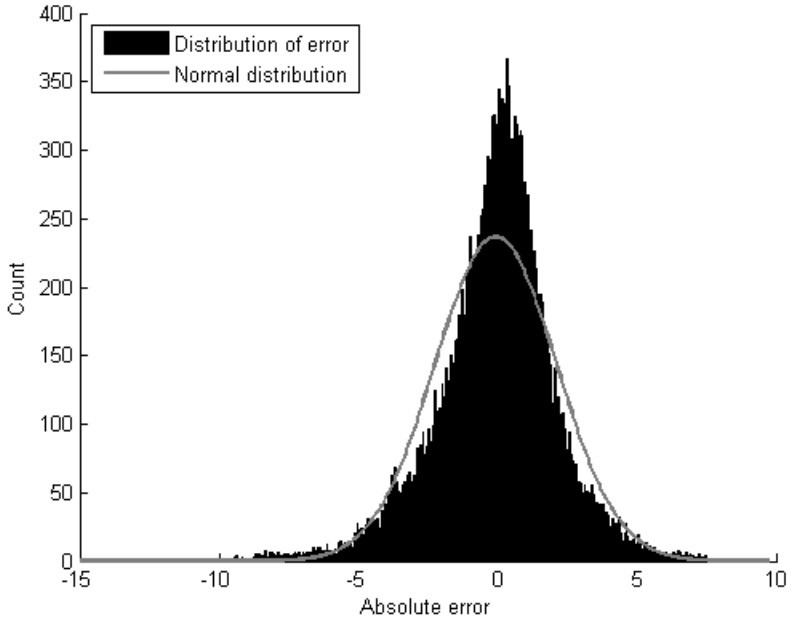

Figure B.4: The absolute error for all nodes of all pins for HBWR.

C Initial guesses

Table 3: The initial guess and the creep rate for the LWR cross sections in the GA.

Cross section	Initial guess	Creep rate	Cross section	Initial guess	Creep rate
$\sigma_{a,Th232}$	3.24	0.05	$\sigma_{c,Th233}$	7.02	0.1
$\sigma_{a,U233}$	126	1	$\sigma_{c,U233}$	8.28	0.1
$\sigma_{a,U234}$	0.418	0.05	$\sigma_{c,U234}$	43.2	1
$\sigma_{a,U235}$	49.1	1	$\sigma_{c,U235}$	4.68	0.3
$\sigma_{a,U236}$	0.0493	0.05	$\sigma_{c,U236}$	35.0	0.5
$\sigma_{a,Pu238}$	9.74	0.5	$\sigma_{c,Pu238}$	150	1
$\sigma_{a,Pu239}$	53.0	1	$\sigma_{c,Pu239}$	30.9	1
$\sigma_{a,Pu240}$	0.0606	0.05	$\sigma_{c,Pu240}$	38.1	1
$\sigma_{a,Pu241}$	43.0	1	$\sigma_{c,Pu241}$	13.6	1
$\sigma_{a,Pu242}$	0.0207	1	$\sigma_{c,Pu242}$	35.3	1

Table 4: The initial guess and the creep rate for the LWR shape function parameters in the GA.

Parameter	Initial guess	Creep rate
$Thp1$	0.530	0.1
$Thp2$	3.67	0.1
$Thp3$	0.835	0.1
$Thp4$	0.466	0.1
$Pup1$	1.08	0.1
$Pup2$	0.837	0.1
$Pup3$	0.850	0.1
$Pup4$	-5.41	0.3
$Pup5$	5.28	0.1
$Pup6$	0	0.1
$Pup7$	8.72	0.5

Table 5: The initial guess and the creep rate for the HBWR cross sections in the GA.

Cross section	Initial guess	Creep rate	Cross section	Initial guess	Creep rate
$\sigma_{a,Th232}$	2.10	0.05	$\sigma_{c,Th233}$	5.71	0.1
$\sigma_{a,U233}$	213	1	$\sigma_{c,U233}$	6.77	0.1
$\sigma_{a,U234}$	1.27	0.05	$\sigma_{c,U234}$	39.3	1
$\sigma_{a,U235}$	56.3	1	$\sigma_{c,U235}$	6.59	0.3
$\sigma_{a,U236}$	0	0.05	$\sigma_{c,U236}$	33.3	0.5
$\sigma_{a,Pu238}$	7.21	0.5	$\sigma_{c,Pu238}$	145	1
$\sigma_{a,Pu239}$	124	1	$\sigma_{c,Pu239}$	96.0	1
$\sigma_{a,Pu240}$	0	0.05	$\sigma_{c,Pu240}$	24.3	1
$\sigma_{a,Pu241}$	174	1	$\sigma_{c,Pu241}$	53.6	1
$\sigma_{a,Pu242}$	0	1	$\sigma_{c,Pu242}$	49.3	1

Table 6: The initial guess and the creep rate for the HBWR shape function parameters in the GA.

Parameter	Initial guess	Creep rate
$Thp1$	0.248	0.1
$Thp2$	1.91	0.1
$Thp3$	0.809	0.1
$Thp4$	0.554	0.1
$Pup1$	0.133	0.1
$Pup2$	0.536	0.1
$Pup3$	0.636	0.1
$Pup4$	-0.311	0.3
$Pup5$	5.41	0.1
$Pup6$	0.0521	0.1
$Pup7$	14.8	0.5